A Classification of Homeostasis Types in Four-node Input-output Networks

Undergraduate Research Thesis

Presented in partial fulfillment of the requirements for graduation *with research distinction* in mathematics in the undergraduate colleges of The Ohio State University

by

Zhengyuan Huang

The Ohio State University
March 2021

Project Advisor: Professor Martin Golubitsky, Department of Mathematics

Abstract

Homeostasis refers to a living system's ability to maintain the steady-state of its internal, physical, or chemical conditions. A system is said to be homeostatic if its output is insensitive to the variations of its input parameter $\mathcal{I}$ over some interval. Homeostasis in a sensory system is often called adaptation [Ma et al. (2009)]. One example of a homeostatic system is the thermoregulation of mammals, in which the body temperatures of mammals are approximately constant over a range of environmental temperatures. [Golubitsky and Stewart (2017), Antoneli et al. (2018), Golubitsky and Wang (2020), Wang et al. (2021)] studied infinitesimal homeostasis, where the input-output function $x_o(\mathcal{I})$ has derivative zero at an isolated point $\mathcal{I}_0$. [Ma et al. (2009)] pointed out that if the number of nodes is fixed, there could be a small amount of network topologies leading to infinitesimal homeostasis. For example, [Reed et al. (2017)] identified two three-node mechanisms which exhibit infinitesimal homeostasis: feed-forward excitation and kinetic homeostasis. Using graph theoretical approach, [Golubitsky and Wang (2020)] assumed the network $\mathcal{G}$ has a designated input-node ι, a designated output-node o, and a third node ρ; they showed the network must have one path (or simple path) from the input node ι to the output node o for infinitesimal homeostasis to exist. Such networks are called input-output networks. Up to core equivalence, they classified 3 three-node input-output networks with distinct types of infinitesimal homeostasis: feed-forward loop, haldane homeostasis, and null-degradation homeostasis.

In this thesis, we extend the results of [Golubitsky and Wang (2020)] to four-node input-output networks. We introduce the concepts of core network and core equivalence, which give a class of minimal networks that can achieve infinitesimal homeostasis. Despite there exists 199 four-node input-output networks, we show up to core equivalence, there are 20 four-node input-output networks. Furthermore, we partitioned the 20 networks (as shown in networks 1-20 of Figures 3 to 5) into three categories: irreducible networks (containing one type of infinitesimal homeostasis), networks with three degree 1 factor (has three different types of infinitesimal homeostasis), and networks with one degree 1 factor and one degree 2 factor (has two different types of infinitesimal homeostasis). We provide a description of how infinitesimal homeostasis can arise in each of the 20 networks and the stability conditions for the steady-state points (a necessary assumption of infinitesimal homeostasis). For instance, network 1 of 3 has three different haldane factors (neutral couplings) and stability condition requires all the internal dynamic terms of the form f_{ℓ,x_ℓ} to be zero. Lastly, we demonstrate our classification theorem with three biochemical networks: intracellular copper regulation, *E. coli* chemotaxis, and allosteric regulation of PFKL/M.

Contents

1 Introduction

Homeostasis refers to the living system's ability to maintain its internal, physical, and chemical conditions. The concept of homeostasis was first mentioned in 1849: French physiologist Claude Bernard wrote in his paper, "all the vital mechanisms, however varied they may be, have only one object, that of preserving constant the condition of life in the internal environment." The term homeostasis was introduced by American physiologist Walter Bradford Cannon in 1926 [Cannon (1926)]. A system is said to be homeostatic if its output parameter remains approximately constant as its input varies. Homeostasis in a sensory or signaling system is called *adaptation*, which allows the sensory output of a system to reset to its basal or near-basal level after responding to an input stimulus.

Many biological processes can achieve adaptation or homeostasis, examples including cellular regulation [Ferrell (2016), Yu et al. (2017)], metabolic signaling pathways [Nijhout et al. (2004), Best et al. (2009), Nijhout and Reed (2014), Nijhout et al. (2015), Nijhout et al. (2018)] bacteria chemotaxis [Barkai and Leibler (1997)], and many more. A classical example of homeostasis is the thermoregulation of mammals studied by [Morrison (1946)]. As shown in Figure 1, the body temperature of brown opossum is held approximately constant when the environmental temperature varies from 10 °C to 30 °C. When environmental temperature gets below 10 °C or above 30 °C, the body temperature of brown opossum seems to be varying linearly; such phenomenon is known as *escape from homeostasis* see [Nijhout et al. (2015)]. [Nijhout and Reed (2014)] called the overall shape of this type of regulations a *homeostasis chair*.

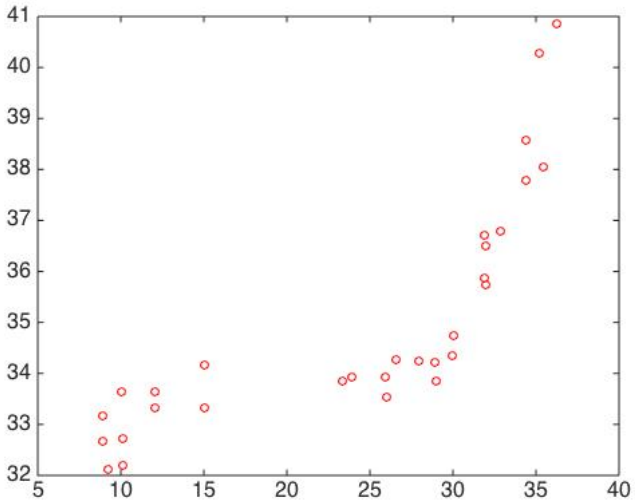

Figure 1: Thermoregulation data of brown opossum from [Morrison (1946)]. The vertical axis indicates the body temperature of brown opossum in degree Celsius; the horizontal axis indicates the environmental temperature.

We summarize the mathematical construction of both homeostasis and adaptation as fol-

lows. To begin, construct a system of ordinary differential equations based on a biochemical network model. Next, define the *input-output function* as the mapping from the system input $\mathcal{I}$ to the system output $x_o(\mathcal{I})$ [Wang et al. (2021)]. One can study the dynamic of $x_0(\mathcal{I})$ by varying the input $\mathcal{I}$ over time to find homeostasis or adaptation in specific networks.

Understanding the mechanisms (network topology) and conditions under which homeostasis is obtained is an active research topic. Many researchers have found recurrent network topologies linked to infinitesimal homeostasis or perfect adaptation. These findings suggest that on fixing the number of nodes, the number of network topologies that can lead to the existence of homeostasis or adaptation is limited. For example, [Reed et al. (2017)] identified two kinds of homeostatic mechanisms in three-node networks: *feedforward excitation* and *kinetic* homeostasis. Similarly, limiting to three-node biochemical networks with Michaelis-Menten rate equations, [Ma et al. (2009)] identified two architectural classes that can achieve adaptation: *negative feedback loop (NFBL)* and *incoherent feedforward loop (IFFL)*.

It is worth noting that the approach taken by [Ma et al. (2009)] involves searching for homeostasis over 16,038 different three-node network models that contain at least one path from the input node to the output node. Figure 2 categorizes the 16,038 networks in terms of topological structures. For each network model, the authors sampled a total of 10,000 sets of parameters and studied the resulting behaviors of the input-output circuits. In total, they analyzed $16,038 * 10,000 \approx 1.6 \times 10^8$ different input-output maps.

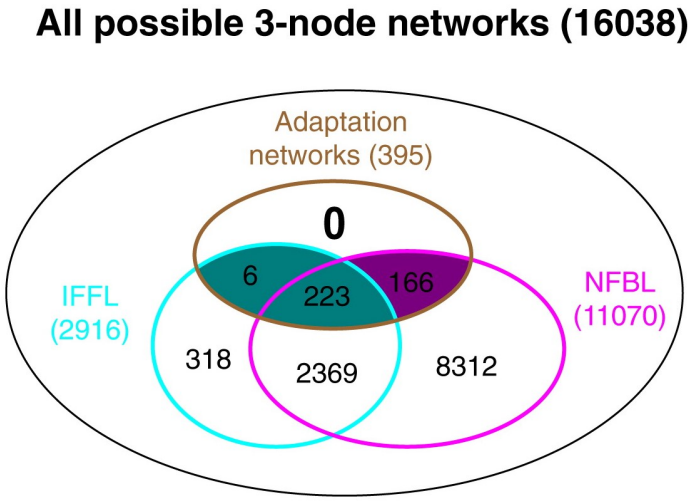

Figure 2: Venn diagram of 16,038 networks with specifying categories from [Ma et al. (2009)].

In the control theory literature, a stronger condition *perfect adaptation* or *robust homeostasis* is widely studied [Ma et al. (2009), Ang and McMillen (2013), Ferrell (2016), Tang and McMillen (2016), Araujo and Liota (2018), Del Vecchio et al. (2018), Aoki et al. (2019)], in which the output can reset exactly to its pre-stimulus level over a broad range of input stimulus. Alternatively, [Golubitsky and Stewart (2017)] introduced the notion of *infinitesimal*

homeostasis, where the derivative of an input-output function $x_o(\mathcal{I})$ is zero at an isolated point $\mathcal{I}_0$. In other words, infinitesimal homeostasis occurs at an isolated point I_0 when $\frac{dx_o}{d\mathcal{I}}(\mathcal{I}_0) = 0$.

[Golubitsky and Wang (2020)] reproduced the results of [Reed et al. (2017), Ma et al. (2009)] using a different approach based on infinitesimal homeostasis. They enumerated all possible three-node networks $\mathcal{G}$ with one node being the designated input node ι, one node being the designated output node o and a regulatory node ρ. They showed that there are 78 different three-node input-output networks, up to *core equivalence* (definition 2.2), only three network topologies can lead to infinitesimal homeostasis: Feed-forward loop, haldane homeostasis, and null-degradation homeostasis.

[Wang et al. (2021)] generalized the setup in [Golubitsky and Wang (2020)] by considering an input-output network $\mathcal{G}$ with one designated input node ι, one designated output node o, and n regulatory nodes. They classified the structures of infinitesimal homeostasis in $\mathcal{G}$. The authors showed that infinitesimal homeostasis can be computed by taking the determinant of a $(n+1) \times (n+1)$ *homeostasis matrix* H (see definition 1.3); specifically, infinitesimal homeostasis occurs at a given point $\mathcal{I}_0$, in other words, $dx_o/d\mathcal{I} = 0$ if and only if $\det(H(\mathcal{I}_0)) = 0$. They then used combinatorial matrix theory to put H into block upper triangular form with diagonal blocks B_j (each B_j is irreducible, namely, no further triangularization can be done). Each diagonal block B_j corresponds to a unique type of infinitesimal homeostasis. In general, the factors fall into two classes: *structural* and *appendage*. Biochemically, structural homeostasis resembles feedforward motifs and appendage homeostasis resembles feedback motifs. The authors also identified two types of degree 1 homeostasis factors (*null-degradation* and *haldane* homeostasis as well as two types of degree 2 homeostasis (*feedforward loop* and *degree two appendage* homeostasis).

In this thesis, we apply the general methods proposed in [Golubitsky and Wang (2020), Wang et al. (2021)] to classify the types of infinitesimal homeostasis in four-node input-output networks. There are a total of 199 connected four-node networks up to relabeling, and over 2000 four-node input-output networks [Harary and Palmer (1973)]. We ask a general question: among the 2000 four-node input-output networks, up to core equivalence, how many of them are capable of infinitesimal homeostasis? To answer this, we introduce the concepts of *core subnetwork* (see definition 2.2), which yields a "minimal network" that is capable of infinitesimal homeostasis. Then, we enumerate all possible four-node core networks up to core equivalence and classify the types of infinitesimal homeostasis that can occur within each network, relating them to the graph-theoretic existence of *simple paths* and *appendage nodes*.

While classifications of infinitesimal homeostasis in a general admissible system provide a global view of homeostasis, four-node input-output networks' study draws a connection between mathematical networks and biological networks. We seek to answer the following questions:

I. Can our classification of four-node infinitesimal homeostasis mechanisms be applied to four-node biochemical networks?

II. Is there an example of a well-studied biochemical network corresponding to each of the 20 four-node homeostasis mechanisms, which exhibits infinitesimal homeostasis?

To address the first question, we give an algorithm for enumerating infinitesimal homeostasis in a four-node biochemical network without doing numerical simulations. We then apply the algorithm to the intracellular copper regulation as shown in Figure 13. For the second question, we demonstrate our results on four-node classification through *E. coli* chemotaxis (see Figure 15) and allosteric regulation of PFKL/M (see Figure 16).

The structure of this thesis is as follows. Section 1.1 defines the concepts of infinitesimal homeostasis, input-output networks, and graph-theoretical terms. In section 2, we introduce the method to compute infinitesimal homeostasis using Cramer's rule. We then introduce the notion of core subnetwork and core equivalence. In section 3, we enumerate all four-node core networks up to core equivalence. In section 4, we present a classification of infinitesimal homeostasis types within four-node input-output networks. In section 5, we address the stability issue and show there is a stable equilibrium for every type of infinitesimal homeostasis among four-node input-output networks. Lastly, section 6 illustrates the application of the four-node classification theorem with three biochemical examples.

1.1 Input-Output Networks and Infinitesimal Homeostasis

The concept of infinitesimal homeostasis has been studied in a series of papers [Golubitsky and Stewart (2017),Reed et al. (2017),Golubitsky and Stewart (2018),Antoneli et al. (2018), Golubitsky and Wang (2020), Wang et al. (2021)]. This thesis is mainly concerned with the classification of four-node infinitesimal homeostasis mechanisms. We review the setup in [Wang et al. (2021)] specialized to the four-node case.

A four-node *input-output network* $\mathcal{G}$ has a distinguished *input node* ι, a distinguished *output node* o, and two *regulatory nodes* ρ, τ. The input-output network $\mathcal{G}$ has a set of arrows connecting the nodes ℓ to nodes j, with at least one path from the input node to the output node. We consider a system ordinary differential equations of the form:

$$\dot{X} = F(X, \mathcal{I}) \tag{1.1}$$

where $X = (x_\iota, x_\rho, x_\tau, x_o) \in \mathbb{R}^4$ are the state variables associated with the nodes, and $\mathcal{I}$ is the *external input parameter*. $F(X, \mathcal{I}) = (f_\iota, f_\rho, f_\tau, f_o)$ is an one-parameter *admissible system* associated with a given network $\mathcal{G}$, where each coordinate function f_ℓ depends on the state variable x_ℓ and the state variables of other nodes that are connected to ℓ.

We make the following assumptions about the vector field F throughout:

(a) Only the coordinate function of the input node f_ι depends on the external input parameter $\mathcal{I}$ and the partial derivative of f_ι with respect to $\mathcal{I}$ cannot be 0 at any point (i.e. $f_{\iota,\mathcal{I}}(X, \mathcal{I}) \neq 0$).

(b) The partial derivative f_{ℓ,x_j} can be nonzero only if $\mathcal{G}$ contains the arrow $j \to \ell$.

(c) F has an asymptotically stable equilibrium at $(X_0, \mathcal{I}_0)$.

It follows from the implicit function theorem and the stability assumption (part (c)) that locally, for each $\mathcal{I}$, there exists a unique function $X(\mathcal{I}) = (x_\iota(\mathcal{I}), x_\rho(\mathcal{I}), x_\tau(\mathcal{I}), x_o(\mathcal{I}))$ such that

$$F(X(\mathcal{I}), \mathcal{I}) \equiv 0 \tag{1.2}$$

with $X(\mathcal{I}_0) = X_0$. We denote $\mathcal{I} \mapsto x_o(\mathcal{I})$ as the *input-output function*. Given a four-node input-output network, the network systems of differential equations of (1.1) have the form

$$\begin{array}{rcl} \dot{x}_\iota &=& f_\iota(x_\iota, x_\rho, x_\tau, x_o, \mathcal{I}) \\ \dot{x}_\rho &=& f_\rho(x_\iota, x_\rho, x_\tau, x_o) \\ \dot{x}_\tau &=& f_\tau(x_\iota, x_\rho, x_\tau, x_o) \\ \dot{x}_o &=& f_o(x_\iota, x_\rho, x_\tau, x_o) \end{array} \tag{1.3}$$

In general, given a four-node input-output network, the corresponding systems of equations will be a subclass of (1.3).

[Golubitsky and Stewart (2017)] introduced the following notion:

Definition 1.1. *Infinitesimal homeostasis* occurs at $\mathcal{I}_0$ if $x_o'(\mathcal{I}_0) = 0$ where $'$ indicates differentiation with respect to $\mathcal{I}$.

If in addition $x_o''(\mathcal{I}_0) = 0$ but $x_o'''(\mathcal{I}_0) \neq 0$, it is called an *infinitesimal chair*; if $x_o''(\mathcal{I}_0) \neq 0$, it is called a *simple homeostasis* or *homeostasis point*.

Couplings in the network systems are defined as follows:

Definition 1.2. Let $F = (f_\iota, f_\rho, f_\tau, f_o)$ be an admissible system for the network $\mathcal{G}$.

(a) The partial derivative $f_{j,x_\ell}(X_0, \mathcal{I}_0)$ is the linearized *coupling* associated with the arrow $\ell \to j$ at the equilibrium $(X_0, \mathcal{I}_0)$.

(b) The partial derivative $f_{j,x_j}(X_0, \mathcal{I}_0)$ is the linearized *self-coupling* of node j at the equilibrium $(X_0, \mathcal{I}_0)$.

(c) The arrow $\ell \to j$ is *excitatory* if $f_{j,x_\ell} > 0$, *inhibitory* if $f_{j,x_\ell} < 0$, and *neutral* if $f_{j,x_\ell} = 0$.

Neutral coupling from ℓ to j can only occur when $\ell \to j$ is an arrow in $\mathcal{G}$.

1.2 Computation of x_o' using Cramer's Rule

[Golubitsky and Wang (2020), Wang et al. (2021)] presented a formula for computing infinitesimal homeostasis points using Cramer's rule.

Definition 1.3. Let J be the 4×4 Jacobian matrix of (1.1) at the equilibrium X_0. H is the 3×3 *homeostasis matrix* obtained by eliminating the first row and the last column of J. Specifically:

$$H = \begin{bmatrix} f_{\rho,x_\iota} & f_{\rho,x_\rho} & f_{\rho,x_\tau} \\ f_{\tau,x_\iota} & f_{\tau,x_\rho} & f_{\tau,x_\tau} \\ f_{o,x_\iota} & f_{o,x_\rho} & f_{o,x_\tau} \end{bmatrix}. \tag{1.4}$$

The following lemma appears in [Golubitsky and Wang (2020), Wang et al. (2021), Ma et al. (2009)].

Lemma 1.4. *Let $(\mathcal{I}_0, X_0)$ be a stable equilibrium for the system (1.1). The input-output function $x_o(\mathcal{I})$ satisfies*

$$x_o'(\mathcal{I}_0) = \pm \frac{f_{\iota,\mathcal{I}}}{\det(J)} \det(H) \tag{1.5}$$

Hence, $\mathcal{I}_0$ is a point of infinitesimal homeostasis (that is, $x_o'(\mathcal{I}_0) = 0$) if and only if

$$\det(H) = 0 \tag{1.6}$$

at $(\mathcal{I}_0, X_0)$.

Proof. Implicit differentiation of (1.2) with respect to $\mathcal{I}$ yields the matrix system

$$J \begin{bmatrix} x_i' \\ x_\rho' \\ x_\tau' \\ x_o' \end{bmatrix} = - \begin{bmatrix} f_{\iota,\mathcal{I}} \\ 0 \\ 0 \\ 0 \end{bmatrix} \tag{1.7}$$

Apply Cramer's rule to (1.7) to solve for x_o' yielding (1.5).

$$x_o'(\mathcal{I}_0) = \frac{1}{\det(J)} \det \begin{bmatrix} f_{\iota,x_\iota} & f_{\iota,x_\rho} & f_{\iota,x_\tau} & -f_{\iota,\mathcal{I}} \\ f_{\rho,x_\iota} & f_{\rho,x_\rho} & f_{\rho,x_\tau} & 0 \\ f_{\tau,x_\iota} & f_{\tau,x_\rho} & f_{\tau,x_\tau} & 0 \\ f_{o,x_\iota} & f_{o,x_\rho} & f_{o,x_\tau} & 0 \end{bmatrix}$$

By assumption, $f_{\iota,\mathcal{I}} \neq 0$ and $\det(J) \neq 0$. Hence, the fact that infinitesimal homeostasis for (1.1) is equivalent to (1.6) follows directly from (1.5). □

Definition 1.5.

A *backward arrow* is an arrow whose head is the input node ι or whose tail is the output node o.

Note that partial derivatives associated with backward arrows do not appear in the matrix H in (1.4).

1.3 Summary of Results

We consider a general network with four nodes (vertices) with unidirectional arrows (edges). There exists $2^{12} = 4096$ four-node networks and up to relabeling, 199 connected four-node networks. We ask the general question: how many different four-node mechanisms lead to the possible existence of infinitesimal homeostasis? To identify the network topologies that can achieve infinitesimal homeostasis, we follow the methods proposed in [Golubitsky and Wang (2020)] and classify infinitesimal homeostasis using general *admissible systems* of a given network. Up to core equivalence, we show there are 20 different four-node mechanisms. We then classify the type of infinitesimal homeostasis within each network and relate them to graph theoretical existence of *simple paths* and *appendage components* (see definition 2.4).

2 Core Network

Even though there are 199 connected four-node networks, there are very few four-node homeostasis mechanisms. [Wang et al. (2021)] showed that for any given input-output network $\mathcal{G}$, there exists a subnetwork $\mathcal{G}_c$ that retains the same homeostasis properties as $\mathcal{G}$ (see theorem 2.3). Formally, $\mathcal{G}_c$ can be obtained from $\mathcal{G}$ by deleting certain nodes and arrows; such network $\mathcal{G}_c$ is called the *core subnetwork*. In addition, if two core networks have the same types of infinitesimal homeostasis, then they are *core equivalent*. The notion of core equivalence is very important when trying to classify infinitesimal homeostasis in four-node networks.

Definition 2.1. Let $\mathcal{G}$ be an input-output network. A node τ in $\mathcal{G}$ is *downstream* from a separate node ρ in $\mathcal{G}$ if there exists a path from ρ to τ. Node τ is *upstream* from node ρ if ρ is downstream from τ.

Note if the output node o in a network $\mathcal{G}$ is not downstream from the input node ι, the input-output function $x_o(\mathcal{I})$ is invariant in $\mathcal{I}$ – a trivial case. In this thesis, we assume the output node o is always downstream from the input node ι to eliminate the trivial possibility. In other words, we assume there exists a path from ι to o.

We now define core network, core subnetwork, core equivalent, and backward arrow.

Definition 2.2. [Wang et al. (2021), Definition 1.7]

(a) An input-output network $\mathcal{G}$ is a *core network* if every node in $\mathcal{G}$ is both upstream from the output node o and downstream from the input node ι.

(b) Let $\mathcal{G}$ be an input-output network. $\mathcal{G}_c$ is called the *core subnetwork* whose nodes are the nodes in $\mathcal{G}$ that are both upstream from the output o and downstream from the input ι and whose arrows are the arrows in $\mathcal{G}$ whose head and tail nodes are both nodes in $\mathcal{G}_c$.

(c) Two core networks are *core equivalent* if the determinants of their homeostasis matrices are identical.

(d) A *backward arrow* is an arrow whose head is the input node ι or whose tail is the output node o.

The next result concerning core networks follows from [Theorem 2.4] of [Wang et al. (2021)].

Theorem 2.3. *[Wang et al. (2021), Theorem 2.4] Let $\mathcal{G}$ be an input-output network and let $\mathcal{G}_c$ be the associated core subnetwork. The input-output function associated with $\mathcal{G}_c$ has a point of infinitesimal homeostasis at $\mathcal{I}_0$ if and only if the input-output function associated with $\mathcal{G}$ has a point of infinitesimal homeostasis at $\mathcal{I}_0$.*

Theorem 2.3 implies that in order to classify infinitesimal homeostasis for networks $\mathcal{G}$, it suffices to classify infinitesimal homeostasis for the core subnetwork $\mathcal{G}_c$.

[Wang et al. (2021)] defined certain graph-theoretic properties concerning core network $\mathcal{G}$ as well as essential results concerning core equivalence:

Definition 2.4. [Wang et al. (2021), Definition 1.15]

(a) A directed path connecting two nodes is a *simple path* if it visits each node on the path exactly once.

(b) An *ιo-simple path* is a simple path connecting the input node ι and the output node o.

(c) A node in $\mathcal{G}$ is *simple* if the node lies on an ιo-simple path and *appendage* if the node is not simple.

(d) The *appendage subnetwork* $A_{\mathcal{G}}$ of $\mathcal{G}$ is the subnetwork consisting of all appendage nodes and all arrows in $\mathcal{G}$ connecting appendage nodes.

(e) The *complementary subnetworks* of an ιo-simple path S is the subnetwork C_S consisting of all nodes not on S and all arrows in $\mathcal{G}$ connecting those nodes.

Theorem 2.5. *[Wang et al. (2021), Theorem 3.2] Two core networks are core equivalent if and only if they have the same set of ιo-simple paths and the Jacobian matrices of the complementary subnetworks to any simple path have the same determinant up to sign.*

Proposition 2.6. *If two core networks differ from each other by the presence or absence of backward arrows, then the core networks are core equivalent.*

Proof. The proof follows directly from theorem 2.5. □

3 Enumeration of Four-node Core Equivalent Classes

It follows from theorem 2.3 that if two networks $\mathcal{G}_1$ and $\mathcal{G}_2$ are core equivalent, then $\mathcal{G}_1$ and $\mathcal{G}_2$ have the same infinitesimal homeostasis types. In this section we classify all four-node networks up to core equivalence.

The four-node core networks are partitioned into three categories: networks without appendage node, networks with one appendage node, and networks with two appendage nodes. Note a four-node input-output $\mathcal{G}$ can have up to two appendage nodes since both the input node ι and the output node o are simple nodes by construction. Up to core equivalence, section 3.1 enumerates all 15 four-node core networks without appendage nodes (see theorem 3.1); section 3.2 shows there are 5 four-node core networks with appendage nodes (see theorem 3.2 and theorem 3.3).

3.1 Four-node Core Networks without Appendage Nodes

In this subsection, we consider all networks $\mathcal{G}$ without any appendage node. Suppose every node in $\mathcal{G}$ is a simple node, then $\mathcal{G}$ can have up to five of the following ιo-simple paths: $\iota \to o$, $\iota \to \rho \to o$, $\iota \to \tau \to o$, $\iota \to \rho \to \tau \to o$, $\iota \to \tau \to \rho \to o$. Proposition 2.6 implies that when classifying homeostasis we can ignore backward arrows. In addition, it follows from

theorem 2.5 that the classification of all core equivalent classes can be done by enumerating all possible sets of simple paths and their corresponding complementary subnetworks.

The following result enumerates 15 different four-node networks without appendage nodes and backward arrows.

Theorem 3.1. *Up to core equivalence (and up to relabeling), there are 15 four-node core networks without backward arrows and appendage nodes; they are shown in Figure 3.*

Proof. Let $\mathcal{G}$ be a four-node core network without backward arrows and appendage nodes. $\mathcal{G}$ can have a minimum of one simple path and a maximum of five simple paths. Theorem 2.5 implies that to classify the 15 four-node core networks up to core equivalence, it suffices to list all possible combinations of simple paths and their corresponding complementary subnetworks of $\mathcal{G}$. Note the pair of simple paths: $\iota \to \rho \to \tau \to o$ and $\iota \to \tau \to \rho \to o$ will give rise to two additional simple paths: $\iota \to \rho \to o$ and $\iota \to \tau \to o$. Also note the complementary subnetworks of $\mathcal{G}$ associated with the simple path $\iota \to o$ have two nodes ρ, τ; thus, the complementary subnetwork associated with $\iota \to o$ can have the following different forms: τ, ρ; $\tau \to \rho$; $\rho \to \tau$; and $\tau \leftrightarrow \rho$.

If $\mathcal{G}$ has only one ιo- simple path S, then both ρ and τ are contained in S; in table 1 we list all possible sets of simple paths and their corresponding complementary subnetworks. Up to relabeling, we obtain 1 network given by network (1) of Figure 3.

Table 1: **One Simple Path**

Simple path (S)	Complementary subnetwork (C_S)
$\iota \to \rho \to \tau \to o$	$\emptyset$
$\iota \to \tau \to \rho \to o$	$\emptyset$

Next, we assume $\mathcal{G}$ has two simple paths. In table 2 we display all possible combinations of simple paths and their corresponding complementary subnetworks. Up to relabeling, it yields five different networks given by networks (2) – (6) of Figure 3.

Table 2: **Two Simple Paths**

(S_1)	(C_{S_1})	(S_2)	(C_{S_2})
$\iota \to o$	$\tau \to \rho$	$\iota \to \tau \to \rho \to o$	$\emptyset$
$\iota \to o$	$\rho \leftrightarrow \tau$	$\iota \to \tau \to \rho \to o$	$\emptyset$
$\iota \to o$	$\rho \to \tau$	$\iota \to \rho \to \tau \to o$	$\emptyset$
$\iota \to o$	$\rho \leftrightarrow \tau$	$\iota \to \rho \to \tau \to o$	$\emptyset$
$\iota \to \rho \to o$	τ	$\iota \to \rho \to \tau \to o$	$\emptyset$
$\iota \to \rho \to o$	τ	$\iota \to \tau \to \rho \to o$	$\emptyset$
$\iota \to \tau \to o$	ρ	$\iota \to \rho \to \tau \to o$	$\emptyset$
$\iota \to \tau \to o$	ρ	$\iota \to \tau \to \rho \to o$	$\emptyset$
$\iota \to \tau \to o$	ρ	$\iota \to \rho \to o$	τ

Suppose $\mathcal{G}$ has three simple paths. In table 3 we enumerate all sets of simple paths (S_1, S_2, S_3) and their complementary subnetworks $(C_{S_1}, C_{S_2}, C_{S_3})$. Up to relabeling, we obtain 6 different networks given by networks $(7) - (12)$ of Figure 3.

Table 3: **Three Simple Paths**

(S_1)	(C_{S_1})	(S_2)	(C_{S_2})	(S_3)	(C_{S_3})
$\iota \to o$	τ, ρ	$\iota \to \tau \to o$	ρ	$\iota \to \rho \to o$	τ
$\iota \to o$	$\tau \to \rho$	$\iota \to \tau \to o$	ρ	$\iota \to \tau \to \rho \to o$	$\emptyset$
$\iota \to o$	$\tau \leftrightarrow \rho$	$\iota \to \tau \to o$	ρ	$\iota \to \tau \to \rho \to o$	$\emptyset$
$\iota \to o$	$\tau \to \rho$	$\iota \to \rho \to o$	τ	$\iota \to \rho \to \tau \to o$	$\emptyset$
$\iota \to o$	$\tau \leftrightarrow \rho$	$\iota \to \rho \to o$	τ	$\iota \to \rho \to \tau \to o$	$\emptyset$
$\iota \to o$	$\tau \to \rho$	$\iota \to \tau \to o$	ρ	$\iota \to \rho \to \tau \to o$	$\emptyset$
$\iota \to o$	$\tau \leftrightarrow \rho$	$\iota \to \tau \to o$	ρ	$\iota \to \rho \to \tau \to o$	$\emptyset$
$\iota \to o$	$\tau \to \rho$	$\iota \to \rho \to o$	τ	$\iota \to \tau \to \rho \to o$	$\emptyset$
$\iota \to o$	$\tau \leftrightarrow \rho$	$\iota \to \rho \to o$	τ	$\iota \to \tau \to \rho \to o$	$\emptyset$
$\iota \to \tau \to o$	ρ	$\iota \to \rho \to o$	τ	$\iota \to \tau \to \rho \to o$	$\emptyset$
$\iota \to \tau \to o$	ρ	$\iota \to \rho \to o$	τ	$\iota \to \rho \to \tau \to o$	$\emptyset$

Assume $\mathcal{G}$ has four simple paths. In table 4 we summarize all possible sets of simple paths (S_1, S_2, S_3, S_4) and their corresponding complementary subnetworks $(C_{S_1}, C_{S_2}, C_{S_3}, C_{S_4})$. Up to relabeling, we obtain two different networks given by networks (13) and (14) of Figure 3.

Table 4: **Four Simple Paths**

(S_1)	(C_{S_1})	(S_2)	(C_{S_2})	(S_3)	(C_{S_3})	(S_4)	(C_{S_4})
$\iota \to o$	$\tau \to \rho$	$\iota \to \tau \to o$	ρ	$\iota \to \rho \to o$	τ	$\iota \to \tau \to \rho \to o$	$\emptyset$
$\iota \to o$	$\tau \to \rho$	$\iota \to \tau \to o$	ρ	$\iota \to \rho \to o$	τ	$\iota \to \rho \to \tau \to o$	$\emptyset$
$\iota \to \tau \to o$	ρ	$\iota \to \rho \to o$	τ	$\iota \to \rho \to \tau \to o$	$\emptyset$	$\iota \to \tau \to \rho \to o$	$\emptyset$

If $\mathcal{G}$ has five simple paths, then there is only one core network as shown in network (15) of Figure 3. $\square$

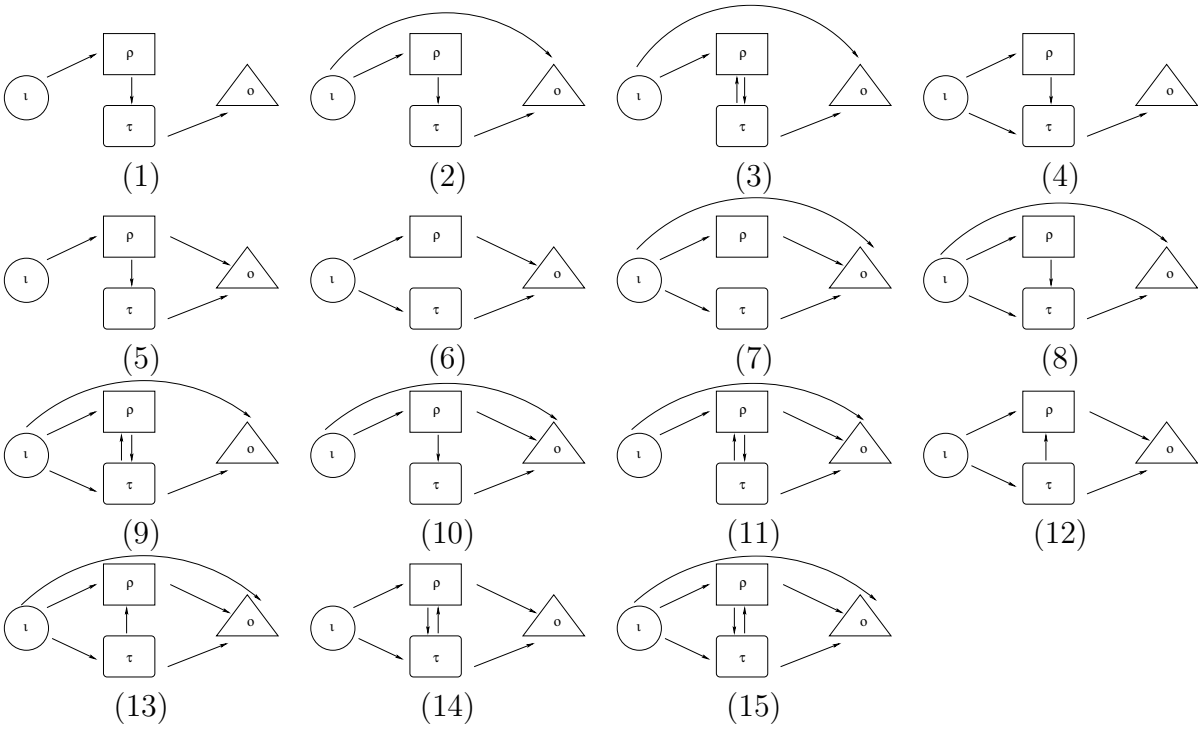

Figure 3: Core networks with no appendage node.

3.2 Four-Node Core Networks with Appendage Nodes

In this section, we classify all four-node core networks with appendage nodes up to core equivalence.

Theorem 3.2. *Up to core equivalence, there are three four-node core networks with one appendage node and they are shown in Figure 4.*

Proof. Let $\mathcal{G}$ be a four-node core network with input node ι, output node o, simple node ρ, and appendage node τ. $\mathcal{G}$ can have two possible ιo- simple paths: $\iota \to o$ and $\iota \to \rho \to o$. We classify all three networks by the number of simple paths in $\mathcal{G}$.

One simple path Suppose $\mathcal{G}$ has only one simple path. Since ρ is a simple node, we have $\iota \to \rho \to o$ as the only simple path of $\mathcal{G}$. Note that the Jacobian matrix of the complementary subnetwork to this simple path is the trivial term f_{τ,x_τ}. It follows from theorem 2.5 that up to core equivalence, there is only one network associated with this simple path, and it is given by network (16) of Figure 4.

Two simple paths Suppose $\mathcal{G}$ has both simple paths: $\iota \to o$ and $\iota \to \rho \to o$. The Jacobian matrix of the complementary subnetwork to the simple path $\iota \to \rho \to o$ contains the internal dynamic f_{τ,x_τ}. However, the Jacobian matrix of the complementary subnetwork

to the simple path $\iota \to o$ is a 2×2 matrix; thus, we obtain two different networks up to core equivalence as shown in Figure 4 (17,18).

□

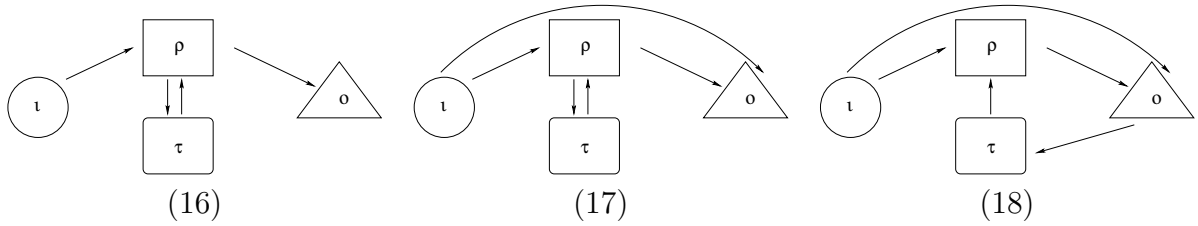

Figure 4: Core networks with one appendage node.

Theorem 3.3. *Up to core equivalence, there are two four-node core networks with two appendage nodes and they are shown in Figure 5.*

Proof. Let $\mathcal{G}$ be a four-node core network with input node ι, output node o, and appendage nodes τ, ρ. The only ιo- simple path is the arrow $\iota \to o$. The Jacobian matrix of the complementary subnetwork to the simple path $\iota \to o$ is a 2×2 matrix; hence, it follows from theorem 2.5, it yields two different networks up to core equivalence given by network (19) and (20) of Figure 5. □

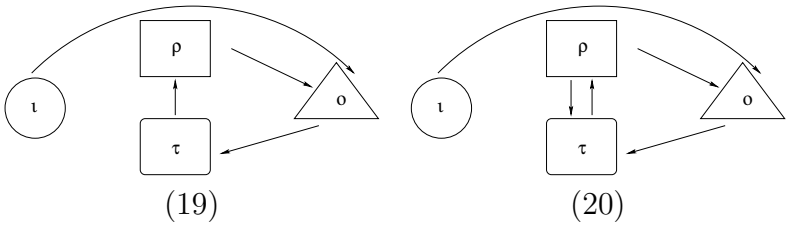

Figure 5: Core networks with two appendage nodes.

4 Classification of Infinitesimal Homeostasis in Four-node Input-output Networks

In this section, we classify the types of infinitesimal homeostasis that can arise in the networks shown in Figures 3 to 5. [Golubitsky and Wang (2020)] defines a *type of infinitesimal homeostasis* as follows: on the vanishing of certain combinations of partial derivatives of $f_\iota, f_\rho, f_\tau, f_o$ (defining conditions), $x'_o(\mathcal{I}_0) = 0, x''_o(\mathcal{I}_0) \neq 0$ holds.

It follows from lemma 1.4 that $x'_o(\mathcal{I}_0) = 0$ is equivalent as $\det(H) = 0$, where H is the homeostasis matrix (see definition 1.3). Thus, infinitesimal homeostasis can be determined

by computing the determinant of the homeostasis matrix H. We now introduce the following notion of reducibility:

Definition 4.1. Let $\mathcal{G}$ be an input-output network with homeostasis matrix H. $\mathcal{G}$ is *irreducible* if $\det(H)$ cannot be factored as a polynomial. $\mathcal{G}$ is *reducible* if $\mathcal{G}$ is not irreducible.

For each core equivalent class, the determinant of the homeostasis matrix $\det(H)$ is a unique polynomial of degree 3. If $\mathcal{G}$ is reducible, then $\det(H)$ can either be written as a product of a degree 1 irreducible polynomial and a degree 2 irreducible polynomial or as a product of three degree 1 irreducible polynomials. [Wang et al. (2021)] proved that each irreducible factor of $\det(H)$ corresponds to a unique type of infinitesimal homeostasis with defined graph-theoretical conditions. We say a type of infinitesimal homeostasis is of *degree* k if it corresponds to an irreducible factor of $\det(H)$ with degree k.

Table 5 lists all the 20 networks, their corresponding homeostasis matrix H, and the determinant of H. The 20 networks can be further partitioned into three categories:

Irreducible networks: Networks 2, 3, 6-15, 17.

Networks with three degree 1 irreducible factors: 1, 16, 19.

Networks with one degree 1 irreducible factor and one degree 2 irreducible factor: 4, 5, 18, 20.

The type of infinitesimal homeostasis associated with four-node irreducible input-output networks is called *structural homeostasis of degree 3*. In general, structural homeostasis does not result from non-neutral couplings and requires a balance of coupling strengths between two or more simple paths (see [Wang et al. (2021)] for more details).

In the remaining of this section, we classify the types of infinitesimal homeostasis among the reducible networks.

Table 5: Enumeration of H matrix and $\det(H)$ for networks in Figures 3 to 5.

Net	H matrix	$\det(H)$
1	$\begin{bmatrix} f_{\rho,x_\iota} & f_{\rho,x_\rho} & 0 \\ 0 & f_{\tau,x_\rho} & f_{\tau,x_\tau} \\ 0 & 0 & f_{o,x_\tau} \end{bmatrix}$	$f_{\rho,x_\iota} f_{\tau,x_\rho} f_{o,x_\tau}$
2	$\begin{bmatrix} f_{\rho,x_\iota} & f_{\rho,x_\rho} & 0 \\ 0 & f_{\tau,x_\rho} & f_{\tau,x_\tau} \\ f_{o,x_\iota} & 0 & f_{o,x_\tau} \end{bmatrix}$	$-f_{o,x_\iota} f_{\rho,x_\rho} f_{\tau,x_\tau} - f_{o,x_\tau} f_{\tau,x_\rho} f_{\rho,x_\iota}$
3	$\begin{bmatrix} f_{\rho,x_\iota} & f_{\rho,x_\rho} & f_{\rho,x_\tau} \\ 0 & f_{\tau,x_\rho} & f_{\tau,x_\tau} \\ f_{\iota,x_\rho} & f_{o,x_\rho} & f_{o,x_\tau} \end{bmatrix}$	$f_{o,x_\iota} f_{\rho,x_\tau} f_{\tau,x_\rho} - f_{o,x_\iota} f_{\rho,x_\rho} f_{\tau,x_\tau} + f_{o,x_\rho} f_{\rho,x_\iota} f_{\tau,x_\tau} - f_{o,x_\tau} f_{\tau,x_\rho} f_{\rho,x_\iota}$

4	$\begin{bmatrix} f_{\rho,x_\iota} & f_{\rho,x_\rho} & 0 \\ f_{\tau,x_\iota} & f_{\tau,x_\rho} & f_{\tau,x_\tau} \\ 0 & 0 & f_{o,x_\tau} \end{bmatrix}$	$f_{o,x_\tau}[f_{\rho,x_\iota}f_{\tau,x_\rho} - f_{\rho,x_\rho}f_{\tau,x_\iota}]$
5	$\begin{bmatrix} f_{\rho,x_\iota} & f_{\rho,x_\rho} & 0 \\ 0 & f_{\tau,x_\rho} & f_{\tau,x_\tau} \\ 0 & f_{o,\rho} & f_{o,x_\tau} \end{bmatrix}$	$f_{\rho,x_\iota}[f_{\tau,x_\rho}f_{o,x_\tau} - f_{\tau,x_\tau}f_{o,x_\rho}]$
6	$\begin{bmatrix} f_{\rho,x_\iota} & f_{\rho,x_\rho} & 0 \\ f_{\tau,x_\iota} & 0 & f_{\tau,x_\tau} \\ 0 & f_{o,x_\rho} & f_{o,x_\tau} \end{bmatrix}$	$-f_{\rho,x_\iota}f_{o,x_\rho}f_{\tau,x_\tau} - f_{o,x_\tau}f_{\tau,x_\iota}f_{\rho,x_\rho}$
7	$\begin{bmatrix} f_{\rho,x_\iota} & f_{\rho,x_\rho} & 0 \\ f_{\tau,x_\iota} & 0 & f_{\tau,x_\tau} \\ f_{o,x_\iota} & f_{o,x_\rho} & f_{o,x_\tau} \end{bmatrix}$	$f_{o,x_\rho}f_{\rho,x_\iota}f_{\tau,x_\tau} + f_{o,x_\tau}f_{\tau,x_\iota}f_{\rho,x_\rho} - f_{o,x_\iota}f_{\rho,x_\rho}f_{\tau,x_\tau}$
8	$\begin{bmatrix} f_{\rho,x_\iota} & f_{\rho,x_\rho} & 0 \\ f_{\tau,x_\iota} & f_{\tau,x_\rho} & f_{\tau,x_\tau} \\ f_{o,x_\iota} & 0 & f_{o,x_\tau} \end{bmatrix}$	$f_{o,x_\iota}f_{\rho,x_\rho}f_{\tau,x_\tau} - f_{\tau,x_\iota}f_{\rho,x_\rho}f_{o,x_\tau} + f_{o,x_\tau}f_{\rho,x_\iota}f_{\tau,x_\rho}$
9	$\begin{bmatrix} f_{\rho,x_\iota} & f_{\rho,x_\rho} & f_{\rho,x_\tau} \\ f_{\tau,x_\iota} & f_{\tau,x_\rho} & f_{\tau,x_\tau} \\ f_{o,x_\iota} & 0 & f_{o,x_\tau} \end{bmatrix}$	$f_{o,x_\iota}f_{\rho,x_\rho}f_{\tau,x_\tau} - f_{\tau,x_\iota}f_{\rho,x_\rho}f_{o,x_\tau} - f_{o,x_\iota}f_{\rho,x_\tau}f_{\tau,x_\rho} + f_{o,x_\tau}f_{\rho,x_\iota}f_{\tau,x_\rho}$
10	$\begin{bmatrix} f_{\rho,x_\iota} & f_{\rho,x_\rho} & 0 \\ 0 & f_{\tau,x_\rho} & f_{\tau,x_\tau} \\ f_{o,x_\iota} & f_{o,x_\rho} & f_{o,x_\tau} \end{bmatrix}$	$f_{o,x_\rho}f_{\rho,x_\iota}f_{\tau,x_\tau} - f_{o,x_\iota}f_{\rho,x_\rho}f_{\tau,x_\tau} - f_{o,x_\tau}f_{\tau,x_\rho}f_{\rho,x_\iota}$
11	$\begin{bmatrix} f_{\rho,x_\iota} & f_{\rho,x_\rho} & f_{\rho,x_\tau} \\ 0 & f_{\tau,x_\rho} & f_{\tau,x_\tau} \\ f_{\iota,x_\rho} & f_{o,x_\rho} & f_{o,x_\tau} \end{bmatrix}$	$f_{o,x_\iota}f_{\rho,x_\tau}f_{\tau,x_\rho} - f_{o,x_\iota}f_{\rho,x_\rho}f_{\tau,x_\tau} + f_{o,x_\rho}f_{\rho,x_\iota}f_{\tau,x_\tau} - f_{o,x_\tau}f_{\tau,x_\rho}f_{\rho,x_\iota}$
12	$\begin{bmatrix} f_{\rho,x_\iota} & f_{\rho,x_\rho} & f_{\rho,x_\tau} \\ f_{\tau,x_\iota} & 0 & f_{\tau,x_\tau} \\ 0 & f_{o,x_\rho} & f_{o,x_\tau} \end{bmatrix}$	$f_{o,x_\rho}f_{\rho,x_\iota}f_{\tau,x_\tau} + f_{o,x_\tau}f_{\tau,x_\iota}f_{\rho,x_\rho} - f_{o,x_\rho}f_{\rho,x_\tau}f_{\tau,x_\iota}$
13	$\begin{bmatrix} f_{\rho,x_\iota} & f_{\rho,x_\rho} & f_{\rho,x_\tau} \\ f_{\tau,x_\iota} & 0 & f_{\tau,x_\tau} \\ f_{o,x_\iota} & f_{o,x_\rho} & f_{o,x_\tau} \end{bmatrix}$	$f_{o,x_\rho}f_{\rho,x_\iota}f_{\tau,x_\tau} - f_{o,x_\iota}f_{\rho,x_\rho}f_{\tau,x_\tau} + f_{o,x_\tau}f_{\tau,x_\iota}f_{\rho,x_\rho} - f_{o,x_\rho}f_{\rho,x_\tau}f_{\tau,x_\iota}$

14	$\begin{bmatrix} f_{\rho,x_\iota} & f_{\rho,x_\rho} & f_{\rho,x_\tau} \\ f_{\tau,x_\iota} & f_{\tau,x_\rho} & f_{\tau,x_\tau} \\ 0 & f_{o,x_\rho} & f_{o,x_\tau} \end{bmatrix}$	$f_{o,x_\rho} f_{\rho,x_\iota} f_{\tau,x_\tau} - f_{o,x_\tau} f_{\tau,x_\rho} f_{\rho,x_\iota} + f_{o,x_\tau} f_{\tau,x_\iota} f_{\rho,x_\rho} - f_{o,x_\rho} f_{\rho,x_\tau} f_{\tau,x_\iota}$
15	$\begin{bmatrix} f_{\rho,x_\iota} & f_{\rho,x_\rho} & f_{\rho,x_\tau} \\ f_{\tau,x_\iota} & f_{\tau,x_\rho} & f_{\tau,x_\tau} \\ f_{o,x_\iota} & f_{o,x_\rho} & f_{o,x_\tau} \end{bmatrix}$	$f_{o,x_\iota} f_{\rho,x_\tau} f_{\tau,x_\rho} - f_{o,x_\iota} f_{\rho,x_\rho} f_{\tau,x_\tau} + f_{o,x_\rho} f_{\rho,x_\iota} f_{\tau,x_\tau} - f_{o,x_\tau} f_{\tau,x_\rho} f_{\rho,x_\iota} + f_{o,x_\tau} f_{\tau,x_\iota} f_{\rho,x_\rho} - f_{o,x_\rho} f_{\rho,x_\tau} f_{\tau,x_\iota}$
16	$\begin{bmatrix} f_{\rho,x_\iota} & f_{\rho,x_\rho} & f_{\rho,x_\tau} \\ 0 & f_{\tau,x_\rho} & f_{\tau,x_\tau} \\ 0 & f_{o,x_\rho} & 0 \end{bmatrix}$	$-f_{\rho,x_\iota} f_{\tau,x_\tau} f_{o,x_\rho}$
17	$\begin{bmatrix} f_{\rho,x_\iota} & f_{\rho,x_\rho} & f_{\rho,x_\tau} \\ 0 & f_{\tau,x_\rho} & f_{\tau,x_\tau} \\ f_{o,x_\iota} & f_{o,x_\rho} & 0 \end{bmatrix}$	$f_{o,x_\iota} f_{\rho,x_\tau} f_{\tau,x_\rho} - f_{o,x_\iota} f_{\rho,x_\rho} f_{\tau,x_\tau} + f_{o,x_\rho} f_{\rho,x_\iota} f_{\tau,x_\tau}$
18	$\begin{bmatrix} f_{\rho,x_\iota} & f_{\rho,x_\rho} & f_{\rho,x_\tau} \\ 0 & 0 & f_{\tau,x_\tau} \\ f_{o,x_\iota} & f_{o,x_\rho} & 0 \end{bmatrix}$	$f_{\tau,x_\tau}[f_{\rho,x_\rho} f_{o,x_\iota} - f_{\rho,x_\iota} f_{o,x_\rho}]$
19	$\begin{bmatrix} 0 & f_{\rho,x_\rho} & f_{\rho,x_\tau} \\ 0 & 0 & f_{\tau,x_\tau} \\ f_{o,x_\iota} & f_{o,x_\rho} & 0 \end{bmatrix}$	$f_{\rho,x_\rho} f_{\tau,x_\tau} f_{o,x_\iota}$
20	$\begin{bmatrix} 0 & f_{\rho,x_\rho} & f_{\rho,x_\tau} \\ 0 & f_{\tau,x_\rho} & f_{\tau,x_\tau} \\ f_{o,x_\iota} & f_{o,x_\rho} & 0 \end{bmatrix}$	$f_{o,x_\iota}[f_{\rho,x_\rho} f_{\tau,x_\tau} - f_{\rho,x_\tau} f_{\tau,x_\rho}]$

4.1 Four-node Core Networks with Degree 1 Factors

In this section, we discuss the types of infinitesimal homeostasis that can occur in networks with three degree 1 irreducible factors. As noted in [Wang et al. (2021)], there are two kinds of degree 1 irreducible factors of $\det(H)$:

Definition 4.2. (a) *Null-degradation homeostasis* corresponds to the vanishing of a degree 1 irreducible factor of the form f_{τ,x_τ}. It arises when the degradation constant of the node τ is zero.

(b) *haldane homeostasis* corresponds to the vanishing of a degree 1 irreducible factor of the form f_{j,x_l}. It arises when the coupling strength of the arrow $\ell \to j$ is neutral.

We relate each homeostasis factor of networks 1, 16, and 19 to its subnetwork as shown in Figures 6 to 8. Haldane arrows are shown in red and null-degradation nodes are shown in cyan.

Theorem 4.3. *Given a four-node input-output network $\mathcal{G}$. Suppose $\mathcal{G}$ is core equivalent to network 1 of Figure 3. Then $\mathcal{G}$ has three haldane factors (neutral couplings). Specifically, infinitesimal homeostasis occurs if and only if one of the following is satisfied:*

(a) $f_{\rho,x_\iota} = 0$, *as shown in Figure 6a.*

(b) $f_{\tau,x_\rho} = 0$, *as shown in Figure 6b.*

(c) $f_{o,x_\tau} = 0$. *as shown in Figure 6c.*

Proof. It follows from lemma 1.4 that infinitesimal homeostasis occurs if and only if $\det(H) = 0$. As shown in Table 5, the determinant of homeostasis matrix is zero if and only if $f_{\rho,x_\iota} f_{\tau,x_\rho} f_{o,x_\tau} = 0$. □

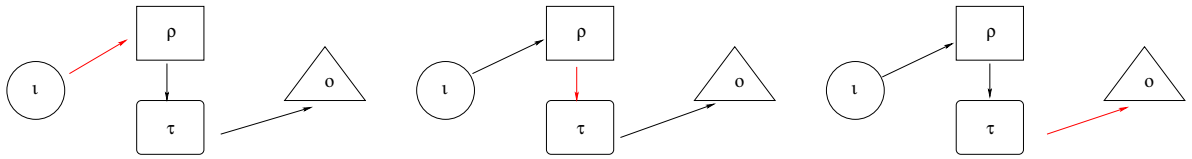

(a) $f_{\rho,x_\iota} = 0$ (b) $f_{\tau,x_\rho} = 0$ (c) $f_{o,x_\tau} = 0$

Figure 6: Subnetworks of network 1; haldane arrows are indicated in red.

Theorem 4.4. *Given a four-node input-output network $\mathcal{G}$. Suppose $\mathcal{G}$ is core equivalent to network 16 of Figure 4. Infinitesimal homeostasis implies either haldane or null-degradation as shown in 7. Specifically:*

(a) Haldane homeostasis occurs if and only if $f_{\rho,x_\iota} = 0$ or $f_{o,x_\tau} = 0$.

(b) Null-degradation homeostasis occurs if and only if $f_{\tau,x_\tau} = 0$.

Proof. It follows from lemma 1.4 that infinitesimal homeostasis occurs if and only if $\det(H) = 0$. As shown in Table 5, the determinant of homeostasis matrix is zero if and only if $f_{\rho,x_\iota} f_{\tau,x_\tau} f_{o,x_\tau} = 0$, as desired. □

Theorem 4.5. *Given a four-node input-output network $\mathcal{G}$. Suppose $\mathcal{G}$ is core equivalent to network 19 of Figure 5. Infinitesimal homeostasis implies either haldane or null-degradation as shown in 7. Specifically:*

(a) Haldane homeostasis occurs if and only if $f_{o,x_\iota} = 0$.

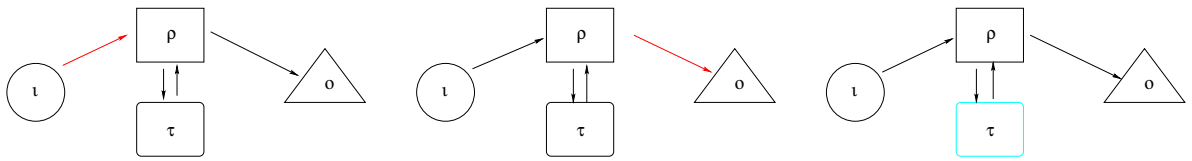

(a) $f_{\rho,x_\iota} = 0$ (b) $f_{o,x_\tau} = 0$ (c) $f_{\tau,x_\tau} = 0$

Figure 7: Subnetworks of network 16; null-degradation factors are indicated in cyan.

(b) Null-degradation homeostasis occurs if and only if $f_{\tau,x_\tau} = 0$ *or* $f_{\rho,x_\rho} = 0$.

Proof. It follows from lemma 1.4 that infinitesimal homeostasis occurs if and only if $\det(H) = 0$. As shown in Table 5, the determinant of homeostasis matrix is zero if and only if $f_{\rho,x_\rho} f_{\tau,x_\tau} f_{o,x_\iota} = 0$, as desired. □

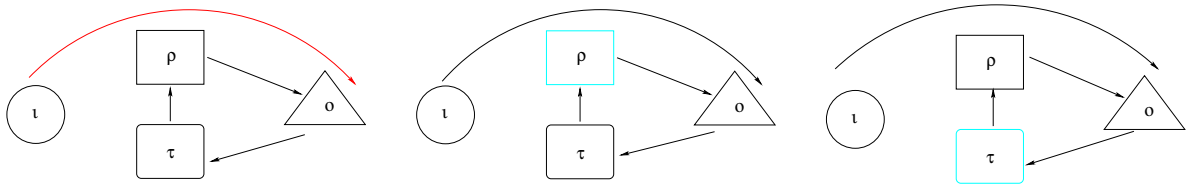

(a) $f_{o,x_\iota} = 0$ (b) $f_{\rho,x_\rho} = 0$ (c) $f_{\tau,x_\tau} = 0$

Figure 8: Subnetworks of network 19.

4.2 Four-node Core Networks with Degree 2 Factors

There are four networks with one degree 2 factor: network 4, 5, 18, 20. [Wang et al. (2021)] identified two kinds of degree 2 factors:

Definition 4.6. (a) *Feed-forward loop* corresponds to the vanishing of a degree 2 irreducible factor of the form:

$$f_{\rho,x_\ell} f_{j,x_\rho} - f_{j,x_\ell} f_{\rho,x_\rho}$$

(b) *Degree 2 no cycle appendage homeostasis* is associated with the vanishing of a degree 2 irreducible factor of the form:

$$f_{\tau_1,x_{\tau_1}} f_{\tau_2,x_{\tau_2}} - f_{\tau_1,x_{\tau_2}} f_{\tau_2,x_{\tau_1}}$$

whose associated subnetwork is a two-node appendage subnetwork with arrows $\tau_1 \to \tau_2$ and $\tau_2 \to \tau_1$.

Remark 4.7. Let $\mathcal{G}$ be a four-node core network. $\mathcal{G}$ has a degree 2 factor if and only if $\mathcal{G}$ has exactly one degree 1 factor.

To indicate homeostasis subnetworks, we redraw the networks 4, 5, 18, 20 as shown in Figures 9 to 12. Feed-forward loop subnetwork is indicated in magenta and degree 2 no cycle appendage subnetwork is indicated in blue.

Theorem 4.8. *Let $\mathcal{G}$ be an input-output four-node network. Suppose $\mathcal{G}$ is core equivalent to network 4 of Figure 3. Infinitesimal homeostasis implies either haldane or feed-forward loop as shown in 9. Specifically:*

(a) Haldane homeostasis occurs if and only if $f_{o,x_\tau} = 0$.

(b) Feed-forward loop occurs if and only if $f_{\rho,x_\iota} f_{\tau,x_\rho} - f_{\rho,x_\rho} f_{\tau,x_\iota} = 0$.

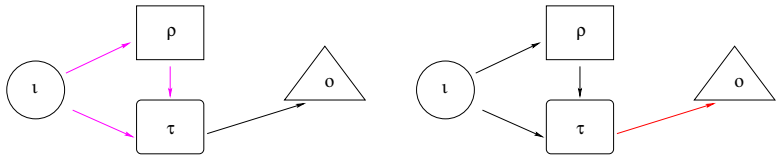

(a) $f_{\rho,x_\iota} f_{\tau,x_\rho} - f_{\rho,x_\rho} f_{\tau,x_\iota} = 0$ (b) $f_{o,x_\tau} = 0$

Figure 9: Subnetworks of network 4, feed-forward loop are indicated in magenta.

Theorem 4.9. *Let $\mathcal{G}$ be an input-output four-node network. Suppose $\mathcal{G}$ is core equivalent to network 5 of Figure 3. Infinitesimal homeostasis implies either haldane or feed-forward loop as shown in 10.*

(a) Haldane homeostasis occurs if and only if $f_{\rho,x_\iota} = 0$.

(b) Feed-forward loop occurs if and only if $f_{\tau,x_\rho} f_{o,x_\tau} - f_{o,x_\rho} f_{\tau,x_\tau} = 0$.

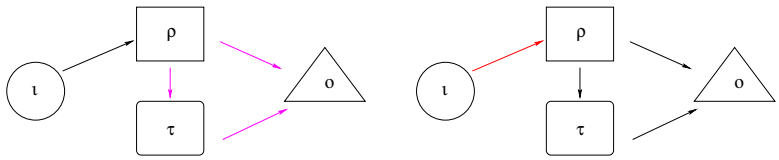

(a) $-f_{\rho,x_\iota} f_{o,x_\rho} + f_{\rho,x_\rho} f_{o,x_\iota} = 0$ (b) $f_{\rho,x_\iota} = 0$

Figure 10: Subnetworks of network 5.

Theorem 4.10. *Let $\mathcal{G}$ be an input-output four-node network. Suppose $\mathcal{G}$ is core equivalent to network 18 of Figure 4. Infinitesimal homeostasis implies either null-degradation or feed-forward loop as shown in 11.*

(a) Null-degradation homeostasis occurs if and only if $f_{\tau,x_\tau} = 0$.

(b) Feed-forward loop occurs if and only if $f_{\rho,x_\rho} f_{o,x_\iota} - f_{\rho,x_\iota} f_{o,x_\rho} = 0$.

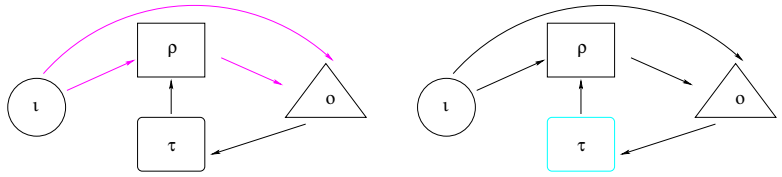

(a) $-f_{\rho,x_\iota}f_{o,x_\rho} + f_{\rho,x_\rho}f_{o,x_\iota} = 0$ (b) $f_{\tau,x_\tau} = 0$

Figure 11: Subnetworks of network 18.

Theorem 4.11. *Let $\mathcal{G}$ be an input-output four-node network. Suppose $\mathcal{G}$ is core equivalent to network 20 of Figure 5. Infinitesimal homeostasis implies either haldane or degree 2 appendage as shown in Figure 12.*

(a) Haldane homeostasis occurs if and only if $f_{o,x_\iota} = 0$.

(b) Degree 2 appendage occurs if and only if $f_{\rho,x_\rho}f_{\tau,x_\tau} - f_{\rho,x_\tau}f_{\tau,x_\rho} = 0$.

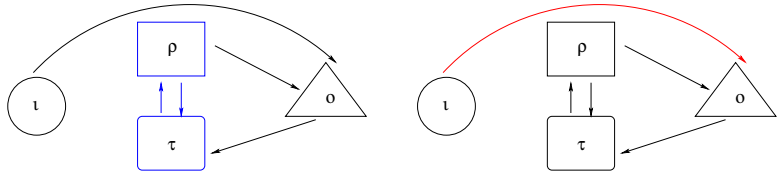

(a) $-f_{\rho,x_\tau}f_{\tau,x_\rho} + f_{\rho,x_\rho}f_{\tau,x_\tau} = 0$ (b) $f_{o,x_\iota} = 0$

Figure 12: Subnetworks of network 20; degree 2 appendage factor is indicated in blue.

5 Stability of Equilibrium and Infinitesimal Homeostasis

In this section, we show for every four-node core network and every form of infinitesimal homeostasis, there exists an equilibrium point such that both stability condition and homeostasis condition are satisfied. First, consider network 17 of figure 4 as an example.

Example 1 Let $\mathcal{G}$ be the network associated with network 17. We assume that infinitesimal homeostasis occurs at a point X_0 when X_0 is a stable equilibrium point. Thus, Jacobian matrix associated with the network must have all negative eigenvalues, where J takes the form of

$$J = \begin{bmatrix} f_{\iota,x_\iota} & 0 & 0 & 0 \\ f_{\rho,x_\iota} & f_{\rho,x_\rho} & f_{\rho,x_\tau} & 0 \\ 0 & f_{\tau,x_\rho} & f_{\tau,x_\tau} & 0 \\ f_{o,x_\iota} & f_{o,x_\rho} & 0 & f_{o,x_o} \end{bmatrix}$$

Observe that f_{ι,x_ι} and f_{o,x_o} are eigenvalues of J. Hence, stability condition implies that both $f_{\iota,x_\iota}, f_{o,x_o} < 0$. In addition, the two remaining eigenvalues are determined by the 2×2 matrix A:

$$A = \begin{bmatrix} f_{\rho,x_\rho} & f_{\rho,x_\tau} \\ f_{\tau,x_\rho} & f_{\tau,x_\tau} \end{bmatrix} \tag{5.1}$$

We see the eigenvalues of A are both negative if $\mathrm{tr}(A) = f_{\rho,x_\rho} + f_{\tau,x_\tau} < 0$ and $\det(A) = -f_{\rho,x_\tau} f_{\tau,x_\rho} + f_{\rho,x_\rho} f_{\tau,x_\tau} > 0$. Recall that infinitesimal homeostasis can occur in $\mathcal{G}$ if

$$\det(H) = +f_{o,x_\iota}[f_{\rho,x_\tau} f_{\tau,x_\rho} - f_{\rho,x_\rho} f_{\tau,x_\tau}] + f_{o,x_\rho} f_{\rho,x_\iota} f_{\tau,x_\tau} = 0$$

Thus, we can assume the internal dynamic terms $f_{\rho,x_\rho}, f_{\tau,x_\tau} < 0$. Note, $\det(H) = 0$ if $f_{o,x_\iota} > 0$ and $f_{o,x_\rho} f_{\rho,x_\iota} < 0$ or $f_{o,x_\iota} < 0$ and $f_{o,x_\rho} f_{\rho,x_\iota} > 0$, i.e. one simple path is excitatory and the other simple path is inhibitory.

We now generalize the results of Example 1 to all irreducible four-node core networks.

Lemma 5.1. *Let $\mathcal{G}$ be an irreducible four-node input-output core network and $S_\mathcal{G}$ be a form of infinitesimal homeostasis exhibited in $\mathcal{G}$. Then, there exists an equilibrium point X_0, such that both stability condition of the system and homeostasis condition of $S_\mathcal{G}$ are satisfied at X_0.*

Proof. Suppose $\mathcal{G}$ is an irreducible four-node core network. It follows from section 4 that on the deletion of backward arrows, $\mathcal{G}$ is still a core network. Suppose $\mathcal{G}$ has no backward arrow, we will show there exists an equilibrium point X_0, such that $\det(H) = 0$.
No backward arrow in $\mathcal{G}$ implies that the Jacobian matrix of $\mathcal{G}$ is block diagonal. Specifically, f_{ι,x_ι} and f_{o,x_o} are eigenvalues of J. Hence, stability condition implies that both $f_{\iota,x_\iota}, f_{o,x_o} < 0$. The two remaining eigenvalues of J are the eigenvalues of A defined by (5.1). Now, we consider two cases:

(i) A is triangular. In other words, at least one of the off-diagonal terms of A is zero. Then stability implies

$$f_{\rho,x_\rho}, f_{\tau,x_\tau} < 0.$$

(ii) A is not triangular. Stability implies that

$$\mathrm{tr}(A) = f_{\rho,x_\rho} + f_{\tau,x_\tau} < 0 \qquad \text{and} \qquad \det(A) = f_{\rho,x_\rho} f_{\tau,x_\tau} - f_{\rho,x_\tau} f_{\tau,x_\rho} > 0$$

Recall that infinitesimal homeostasis can arise in a four-node irreducible core network by balancing of the nonzero summands of associated with more than one simple paths as shown in table 5. If we let the internal dynamic terms be negative in both cases, then there exists a stable equilibrium point X_0 such that $\det(H) = 0$. □

It remains to show the stability conditions for the reducible core networks (that is networks with either three degree 1 factors or one degree 2 factor).

Example 2 Let $\mathcal{G}$ be the network associated with network 1. Recall that infinitesimal homeostasis occurs if and only if $f_{\rho,x_\iota} = 0$ or $f_{\tau,x_\rho} = 0$ or $f_{o,x_\tau} = 0$.
We see that $\mathcal{G}$ has no backward arrow. In addition, the matrix A defined by (5.1) is triaugular. Stability condition implies that all internal dynamic terms are negative.

Example 3 Let $\mathcal{G}$ be the network associated with network 16. We see that $\mathcal{G}$ has no backward arrow. In addition, the matrix A defined by (5.1) is not triaugular. Stability condition implies that $\text{tr}(A) = f_{\rho,x_\rho} + f_{\tau,x_\tau} < 0$ and $\det(A) = -f_{\rho,x_\tau} f_{\tau,x_\rho} + f_{\rho,x_\rho} f_{\tau,x_\tau} > 0$ and $f_{\iota,x_\iota}, f_{o,x_o} < 0$. Recall that

(a) haldane homeostasis occurs if and only if $f_{\rho,x_\iota} = 0$ or $f_{o,x_\tau} = 0$.

(b) Null-degradation homeostasis occurs if and only if $f_{\tau,x_\tau} = 0$. In addition, stability of equilibrium implies $f_{\rho,x_\rho} < 0$ and $f_{\rho,x_\tau} f_{\tau,x_\rho} > 0$.

Example 4 Let $\mathcal{G}$ be the network associated with network 19. We see that $\mathcal{G}$ requires backward arrow. The jacobian matrix of $\mathcal{G}$ takes the form:

$$J = \begin{bmatrix} f_{\iota,x_\iota} & 0 & 0 & 0 \\ 0 & f_{\rho,x_\rho} & f_{\rho,x_\tau} & 0 \\ 0 & 0 & f_{\tau,x_\tau} & f_{\tau,x_o} \\ f_{o,x_\iota} & f_{o,x_\rho} & 0 & f_{o,x_o} \end{bmatrix}$$

Recall that

(a) haldane homeostasis occurs if and only if $f_{o,x_\iota} = 0$. Suppose $f_{o,x_\rho} = 0$, then there exists a stable equiblibrium point X_o where all internal dynamic terms are negative.

(b) Null-degradation homeostasis occurs if and only if $f_{\tau,x_\tau} = 0$ or $f_{\rho,x_\rho} = 0$. Case I: $f_{\tau,x_\tau} = 0$. Stability condition implies that there exists a stable equilibrium X_o satisfying $f_{\iota,x_\iota} < 0$, $f_{\rho,x_\rho} + f_{o,x_o} < 0$, and $f_{\rho,x_\tau} f_{\tau,x_o} f_{o,x_\rho} < 0$. Case II: $f_{\rho,x_\rho} = 0$. Stability condition implies that there exists a stable equilibrium X_o satisfying $f_{\iota,x_\iota} < 0$, $f_{\tau,x_\tau} + f_{o,x_o} < 0$, and $f_{\rho,x_\tau} f_{\tau,x_o} f_{o,x_\rho} < 0$.

Example 5 Let $\mathcal{G}$ be the network associated with network 4. Recall that:

(a) haldane homeostasis occurs if and only if $f_{o,x_\tau} = 0$.

(b) Feed-forward loop occurs if and only if $f_{\rho,x_\iota} f_{\tau,x_\rho} - f_{\rho,x_\rho} f_{\tau,x_\iota} = 0$.

We see that $\mathcal{G}$ has no backward arrow. In addition, the matrix A defined by (5.1) is triaugular. Stability condition implies that all internal dynamic terms are negative.

Example 6 Let $\mathcal{G}$ be the network associated with network 5. Recall that:

(a) haldane homeostasis occurs if and only if $f_{\rho,x_\iota} = 0$.

(b) Feed-forward loop occurs if and only if $f_{\tau,x_\rho}f_{o,x_\tau} - f_{o,x_\rho}f_{\tau,x_\tau} = 0$.

We see that $\mathcal{G}$ has no backward arrow. In addition, the matrix A defined by (5.1) is triaugular. Stability condition implies that all internal dynamic terms are negative.

Example 7 Let $\mathcal{G}$ be the network associated with network 18. We see that $\mathcal{G}$ requires backward arrow. The jacobian matrix of $\mathcal{G}$ takes the form:

$$J = \begin{bmatrix} f_{\iota,x_\iota} & 0 & 0 & 0 \\ f_{\rho,x_\iota} & f_{\rho,x_\rho} & f_{\rho,x_\tau} & 0 \\ 0 & 0 & f_{\tau,x_\tau} & f_{\tau,x_o} \\ f_{o,x_\iota} & f_{o,x_\rho} & 0 & f_{o,x_o} \end{bmatrix}$$

Recall that:

(a) Null-degradation homeostasis occurs if and only if $f_{\tau,x_\tau} = 0$. Stability condition implies that there exists a stable equilibrium X_o satisfying $f_{\iota,x_\iota} < 0$, $f_{\rho,x_\rho} + f_{o,x_o} < 0$, and $f_{\rho,x_\tau}f_{\tau,x_o}f_{o,x_\rho} < 0$.

(b) Feed-forward loop occurs if and only if $f_{\rho,x_\rho}f_{o,x_\iota} - f_{\rho,x_\iota}f_{o,x_\rho} = 0$. There exists a stable equilibrium such that $f_{\iota,x_\iota} < 0$, $f_{\rho,x_\rho} + f_{\tau,x_\tau} + f_{o,x_o} < 0$ and $f_{\rho,x_\rho}f_{\tau,x_\tau}f_{o,x_o} - f_{\rho,x_\tau}f_{\tau,x_o}f_{o,x_\rho} < 0$.

Example 8 Let $\mathcal{G}$ be the network associated with network 20. We see that $\mathcal{G}$ requires backward arrow. The jacobian matrix of $\mathcal{G}$ takes the form:

$$J = \begin{bmatrix} f_{\iota,x_\iota} & 0 & 0 & 0 \\ 0 & f_{\rho,x_\rho} & f_{\rho,x_\tau} & 0 \\ 0 & f_{\tau,x_\rho} & f_{\tau,x_\tau} & f_{\tau,x_o} \\ f_{o,x_\iota} & f_{o,x_\rho} & 0 & f_{o,x_o} \end{bmatrix}$$

Recall that:

(a) haldane homeostasis occurs if and only if $f_{o,x_\iota} = 0$. Suppose $f_{\tau,x_o} = f_{\rho,x_\tau} = 0$. There exist a stable equilibrium point X_o satisfying all internal dynamics are negative.

(b) Degree 2 appendage occurs if and only if $f_{\rho,x_\rho}f_{\tau,x_\tau} - f_{\rho,x_\tau}f_{\tau,x_\rho} = 0$. Stability condition implies that there exists a stable equilibrium X_o satisfying $f_{\iota,x_\iota} < 0$, $f_{\rho,x_\tau}f_{\tau,x_o}f_{o,x_\rho} < 0$, and $f_{\rho,x_\rho} + f_{\tau,x_\tau} + f_{o,x_o} < 0$.

6 Examples of Four-node Biochemical Input-Output Networks

In this section we demonstrate our classification results with three biochemical networks. We ask a general question: can the classification theory of four-node homeostasis mechanisms be

applied to any four-node biochemical network? The answer to this question is yes, however, in order to apply the theoretical results, the core input-output subnetwork $\mathcal{G}_c$ must have four nodes with one designated input node, one designated output node, and two regulatory nodes.

In subsection 6.1 we derive an algorithm for computing homeostasis in an applicable four-node biological network without using numerical simulations. Subsection 6.2 applies the algorithm to the intracellular copper regulation network as shown in figure 13. Subsection 6.3 and subsection 6.4 provide two examples of well-known biochemical networks: *E. coli* chemotaxis network (figure 15) and allosteric regulation of PFKL/M (figure 16). The corresponding core input-output subnetworks of both examples are core equivalent to one of the 20 four-node core equivalent classes. Using the classification theory, we show our predictions on how infinitesimal homeostasis can arise in each network agree with the literature.

6.1 Algorithm for computing homeostasis in a biological network

To compute infinitesimal homeostasis in a biochemical model, we apply the following algorithm.

Step 1: Identify the input node, output node, ιo-simple paths, and appendage nodes. Then, convert the biological network into an input-output core subnetwork $\mathcal{G}_c$.

Step 2: Associate the four-node input-output core subnetwork $\mathcal{G}_c$ with one of the 20 classes discussed in section 3. Check the conditions of infinitesimal homeostasis using the theorems stated in section 4.

(Note this procedure may require removal or addition of backward arrows and renumbering of nodes.)

Step 3: Check the stability conditions using results from section 5.

6.2 Intracellular Copper Homeostasis

In this section, we apply the algorithm in subsection 6.1 to the intracellular copper regulation system studied by [Andrade et al. (2021)]. The four-node biochemical network of intracellular copper regulation is shown in figure 13a.

Copper is an essential cofactor in many physiological processes, such as wound healing, neurotransmitter synthesis, modulation of normal cell and tumor growth, etc [Witt et al. (2020), Yu et al. (2017), Lutsenko et al. (2006)]. The concentration of intracellular copper needs to be strictly regulated since abnormal level of copper can lead to severe consequences. For example, deficiency of copper is linked to Menkes disease [Kodama (1993)], and overload of copper is linked to Wilson disease [Yu et al. (2017)].

Extracellular copper (Cu_{ext}) enters the cell mainly via the copper transport receptor 1 (CTR1). In the cytosol, copper (Cu_{cyt}) is rapidly incorporated into glutathione, from where

it is attached to antioxidant protein-1 (ATOX-1). ATOX-1 protein takes the cytosolic copper to two copper transporting ATPases: ATP7A and ATP7B. These use ATP to pump copper to trans-Golgi network (Cu_{TG}), also known as copper secretory pathway. When Cu_{cyt} is low, ATP7A and ATP7B transfer Cu ions from Cu_{TG} to ATOX-1. The transporters ATP7A and ATP7B play key roles in regulating copper homeostasis ([Lutsenko et al. (2006)]). In response to high level of intracellular copper, ATP7A and ATP7B can translocate from golgi network to cell membrane and release copper into the plasma.

We now apply the three steps of the algorithm:

1. In this example, Cu_{ext} is the input node, Cu_{cyt} is the output node, and ATOX1 and Cu_{TG} are appendage nodes. Figure 13 shows the four-node intracellular copper regulation network (13a) and the corresponding input-output network $\mathcal{G}$ (13b). The four-node input-output network $\mathcal{G}$ associated to intracellular copper regulation network has one ιo-simple path $\iota \to o$ and one appendage path component.

(a) Intracellular copper regulation network.

(b) The input-output network $\mathcal{G}$ corresponding to Figure 13a

Figure 13: **Intracellular Copper Regulation System.**

2. The input-output network $\mathcal{G}$ takes the same form as network 20. By theorem 4.11, infinitesimal homeostasis is possible in $\mathcal{G}$ if either $f_{o,x_\iota} = 0$ or $f_{\rho,x_\rho} f_{\tau,x_\tau} - f_{\rho,x_\tau} f_{\tau,x_\rho} = 0$ is satisfied. Using the classification theorem, we computed homeostasis condition in a intracellular copper regulation model studied by [Andrade et al. (2021)]:

$$\begin{array}{rclcl} \dot{x}_\iota &=& \mathcal{I} - k_0 x_\iota & = & f_\iota(x_\iota, \mathcal{I}) \\ \dot{x}_\rho &=& g k_3 x_\tau + \omega_2 \frac{x_\tau(x_\rho - x_\tau)}{1+x_\tau} - k_4 x_\rho & = & f_\rho(x_\rho, x_\tau) \\ \dot{x}_\tau &=& f k_1 x_o - k_3 x_\tau - \omega_2 \frac{x_\tau(x_\rho - x_\tau)}{1+x_\tau} & = & f_\tau(x_\rho, x_\tau, x_o) \\ \dot{x}_o &=& \frac{k_0}{N} x_\iota - k_1 x_o(1 + \omega_1 x_o) + k_2 G(x_\rho) & = & f_o(x_\iota, x_\rho, x_o) \end{array} \tag{6.1}$$

where $N, f, g, \omega_1, \omega_2, k_0, k_1, k_2, k_3, k_4$ are positive constants, and $G(x_\rho)$ is a quadratic Hill function given by:

$$G(x) = \frac{1}{1+x^2} - 1$$

Therefore, infinitesimal homeostasis can occur if

$$0 = -f_{\rho,x_\tau} f_{\tau,x_\rho} + f_{\rho,x_\rho} f_{\tau,x_\tau} = k_4 \left(k_3 + \omega_2 \frac{x_\rho - 2x_\tau - {x_\tau}^2}{(1+x_\tau)^2} \right) + (g-1) k_3 \omega_2 \frac{x_\tau}{1+x_\tau} \quad (6.2)$$

or

$$0 = f_{o,x_\iota} = \frac{k_0}{N} \quad (6.3)$$

Note $\frac{k_0}{N} > 0$; so, infinitesimal homeostasis occurs if and only if (6.2) is satisfied.

3. It follows from example 8 that there exists a stable equilibrium point satisfying

$$f_{\iota,x_\iota} < 0 \qquad f_{\rho,x_\tau} f_{\tau,x_o} f_{o,x_\rho} < 0 \qquad f_{\rho,x_\rho} + f_{\tau,x_\tau} + f_{o,x_o} < 0.$$

Using the set of parameters obtained from [Andrade et al. (2021)], we show infinitesimal homeostasis point occurs at an stable equilibrium point $\mathcal{I}_0 = 4.7$ as shown in Figure 14.

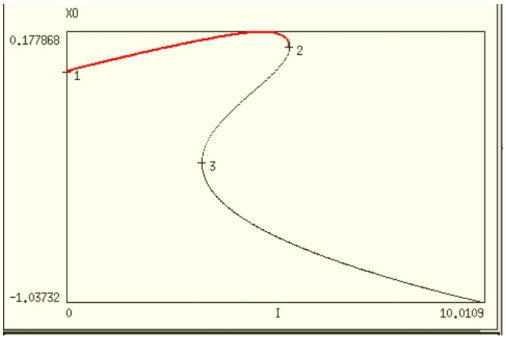

Figure 14: The bifurcation diagram depicting input-output map x_o (y-axis) corresponding to intracellular copper regulation as a function of input parameter $\mathcal{I}$ (x-axis). Red line indicates stable equilibrium and black line indicates unstable equilibrium. Infinitesimal homeostasis point occurs at $\mathcal{I}_0 = 4.7$, and bifurcation point occurs at $\mathcal{I}_0 = 5.2$. The parameter values are: $N = 10$, $f = 0.5$, $g = 0.05$, $\omega_1 = 1$, $\omega_2 = 0.5$, $k_0 = 10$, $k_1 = 2$, $k_2 = 1$, $k_3 = 0.5$, $k_4 = 1$.

6.3 *Escherichia Coli* Chemotaxis

Chemotaxis is the movement of bacterial species toward the attractions of certain chemicals necessary for their survival. The movement of a swimming bacterium consists of 'smooth run' and 'tumbles' (switch direction) [Barkai and Leibler (1997)]. Bacterium is able to swim towards attractants or flee away from poisons by changing its tumbling frequency. Chemotaxis of *Escherichia coli* (*E. coli*) is a well-studied example of infinitesimal homeostasis: the steady-state of tumbling frequency is invariant under the change of ligand concentrations. In this way, *E. coli* can better respond (more sensitive) to the chemical stimulus over a broad range of attractants/repellent concentrations.

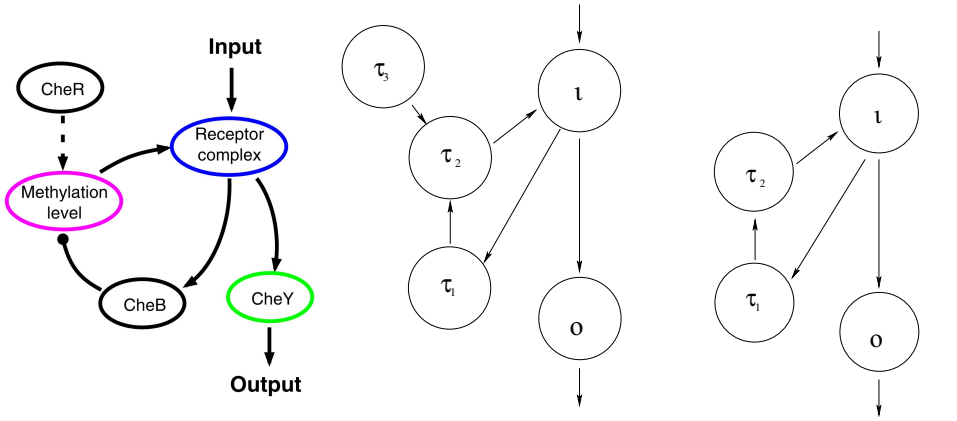

(a) The *E. coli* chemotaxis network from [Ma et al. (2009)].

(b) The mathematical input-output network $\mathcal{G}$ corresponding to *E. coli* network.

(c) The core network $\mathcal{G}_c$ of $\mathcal{G}$.

Figure 15: **The Network of Infinitesimal Homeostasis in *E. coli* chemotactic cells.**

E. coli chemotactic response is conducted through a network system known as the intracellular signaling pathway (as shown in Figure 15a) [Barkai and Leibler (1997), Ma et al. (2009), Edgington and Tindall (2018)]. The intracellular signaling pathway can be summarized as follows: *E. coli* cells sense the environment via chemoreceptors which contain a histidine kinase CheA and a linker protein CheW. When no attractant gradient is detected, CheA autophosphorylates to form CheA-P [Edgington and Tindall (2018)]. The phosphoryl groups can then be transferred to either CheY (the response regulator) or CheB (the methylesterase). When phosphoryl groups are transferred to CheY, it autophosphorylates to form CheY-P. CheY-P regulates the flagellar motor and generates tumbling [Barkai and Leibler (1997)]. The autophosphorylation of receptor complex is regulated by its methylation level in the following way: the protein CheR constantly methylates the receptor, which increases kinase activity, while CheB demethylates the receptor [Barkai and Leibler (1997), Edgington and Tindall (2018)]. The balance of these processes enables CheA or the receptor complex as well as CheY-P to return to their prestimulus values.

Figure 15b shows the five-node mathematical network $\mathcal{G}$ corresponding to the *E. coli* chemotaxis network, where the input node ι is *receptor complex* and the output node o is *CheY*. Furthermore, we can reduce $\mathcal{G}$ to a 4-node core network $\mathcal{G}_c$ (as shown in figure 15c) by removing the node τ_3, which is not downstream from ι and the arrow $\tau_3 \to \tau_2$. The remaining nodes form a core network by definition 2.1. The core network $\mathcal{G}_c$ has one ιo-simple path $\iota \to o$, and two appendage nodes τ_1 (CheB) and τ_2 (Methylation level).

The input-output core network $\mathcal{G}_c$ takes the same form (up to core equivalence) as network 19. It follows from theorem 4.5 that infinitesimal homeostasis is possible in $\mathcal{G}_c$ if either $f_{o,x_\iota} = 0$, $f_{\tau_1,x_{\tau_1}} = 0$, or $f_{\tau_2,x_{\tau_2}} = 0$ is satisfied.

[Barkai and Leibler (1997), Ma et al. (2009)] observed that perfect adaptation occurs in $\mathcal{G}_c$ provided $f_{\tau_2,x_{\tau_2}} = 0$. In other words, the activity of CheY-p in *E. Coli* chemotaxis

network is modulated by the concentration of methylation level.

6.4 Allosteric Regulation of PFKL/M

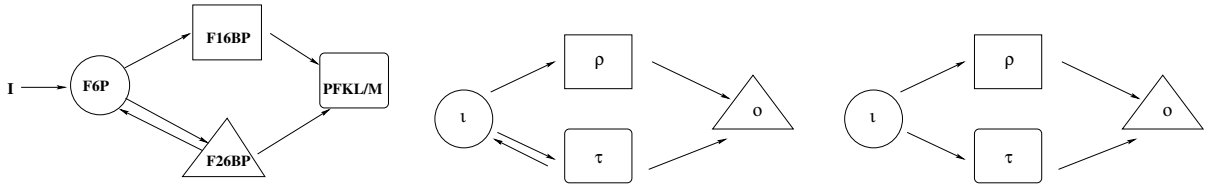

(a) Allosteric regulation of PFKL/M from [Mulukutla et al (2014)]

(b) The input-output network $\mathcal{G}$ corresponding to Figure 16a

(c) Core equivalent to Figure 16b

Figure 16: **Allosteric Regulation in F6P-node.**

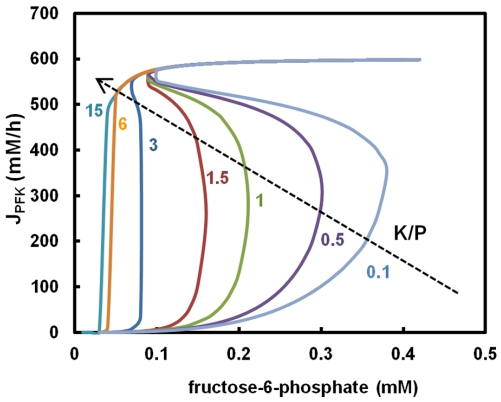

Figure 17: **Concentration of PFK vs F6P**

Figure 16 shows the four node network associated with the allosteric regulation of PFKL/M within the glycolysis pathway [Mulukutla et al (2014)].

Glycolysis describes a very important metabolic pathway. The main function of glycolysis involves converting glucose into pyruvate. The flux of glycolysis activity is tightly controlled through different levels of regulations [Mulukutla et al (2014)]. One pivotal regulation is played by the enzyme phosphofructokinase (PFK). The PFK enzyme has three isoforms: PFKL (liver), PFKM (muscle), and PFKP (platelet); all three isoforms are activated by the protein fructose-6-phosphate (F6P), but only PFKM and PFKL can be activated by fructose-1,6-bisphosphate (F16BP).

[Mulukutla et al (2014)] showed that the concentration of PFKL/M remains homeostatic as the concentration of F6P varies. Figure 16a shows the allosteric regulation network associated with PFKL/M. F6P acts as an input node, it activates both F16BP and F26BP nodes.

In return, F26BP can modulate the F6P-node steady-state behavior. Lastly, PFKL/M is activated by the proteins F26BP and F16BP.

Figure 16b shows the four-node mathematical network $\mathcal{G}$ corresponds to Figure 16a, where the input node ι is F6P, output node o is PFKL/M, and regulatory nodes ρ, τ are F16BP and F26BP. We see the network $\mathcal{G}$ is core equivalent to Figure 16c (network 6), which has two simple paths $\iota \to \rho \to o$ and $\iota \to \tau \to o$. It follows from table 5 that the system exhibits infinitesimal homeostasis if $-f_{\rho,x_\iota} f_{o,x_\rho} f_{\tau,x_\tau} - f_{o,x_\tau} f_{\tau,x_\iota} f_{\rho,x_\rho} = 0$.

As shown in Figure 17, the concentration of PFKL/M enzyme is approximately constant as the concentration of F6P node varies. Additionally, [Mulukutla et al (2014)] proved that when no other allosteric regulation is present in the glycolysis pathway, the steady-state of glycolysis flux exhibits homeostasis when PFKL/M is activated.

7 Conclusion

In this thesis we enumerate all possible four-node homeostasis mechanisms. We assume the four-node network $\mathcal{G}$ has a distinguished input node ι, a distinguished output node o, and two regulatory nodes ρ, τ. Then, we introduce the notion of core and core equivalence. In doing this, the number of distinct four-node input-output networks with the ability to achieve homeostasis or adaptation is significantly reduced. We show up to core equivalence, there are 20 four-node input-output networks.

As previously proved by [Golubitsky and Wang (2020), Wang et al. (2021)], infinitesimal homeostasis in a given network can be computed using the determinant of its homeostasis matrix. Given an input-output network, we call it irreducible if the determinant of its homeostasis matrix cannot be factored as a polynomial; otherwise, it is called reducible. The 20 classes of four-node core equivalent networks can be partitioned into three categories: irreducible networks, networks with three degree 1 irreducible factors, and networks with one degree 1 irreducible factor and one degree 2 irreducible factor.

For each four-node irreducible network, only one type of infinitesimal homeostasis can occur: structural homeostasis of degree 3 [Wang et al. (2021)]. Although it is still unclear how structural homeostasis arises in different four-node irreducible networks, in general, it requires a balance of coupling strengths among two or more simple paths. We enumerate all types of infinitesimal homeostasis within each reducible four-node networks. Specifically, each factor of the determinant of homeostasis matrix corresponds to a unique type of infinitesimal homeostasis, and can be related to a subgraph or subnetwork (see [Wang et al. (2021)] for more). Moreover, we show there exists a stable equilibrium point for every infinitesimal homeostasis type of four-node networks.

We demonstrate our classification results with examples from biochemical networks. First, we provide an algorithm of finding homeostasis points within biochemical networks, whose core subnetwork has four-nodes. We apply the algorithm to the intracellular copper regulation network. Then, we provide two well-studied examples of four-node biochemical networks which can achieve infinitesimal homeostasis: *E. coli* chemotaxis [Barkai and Leibler (1997), Ma et al. (2009), Edgington and Tindall (2018)] and allosteric regulation of PFKL/M

node [Mulukutla et al (2014)]. We show the mathematical network of *E. coli* chemotaxis is core equivalent to network 19 while the network of allosteric regulatioin of PFKL/M is core equivalent to network 6. Using the four-node classification theorem, we predict the conditions on which infinitesimal homeostasis can arise in each biochemical network. We show our theoretical results agree with the literature.

Our thesis comes with certain limitations. Here are some points to consider for future work:

(1) What can we say about the different types of structural homeostasis of degree 3 (corresponding to four-node irreducible networks)?

(2) Can codimension 2 homeostasis be found in four-node networks?

(3) Is it possible to extend the classification theorem of one-input / one-output networks to multi-input / multi-output networks?

The answer to the first question is yet to be known. [Golubitsky and Wang (2020)] indicated structural homeostasis typically requires some simple paths to be excitatory and some to be inhibitory such that the coupling strengths are balanced. One possible direction is to study more examples of biochemical networks associated with four-node irreducible networks. Question (2) has partially been studied in recent work. Some progress toward the answer to question (3) has been made in the case of multi-input / single-output networks (see [Golubitsky and Stewart (2018), Madeira and Antoneli]).

References

[Ang and McMillen (2013)] J. Ang and D.R. McMillen. Physical constraints on biological integral control design for homeostasis and sensory adaptation. *Biophys. J.* **104** (2) (2013) 505–515.

[Antoneli et al. (2018)] F. Antoneli, M. Golubitsky and I. Stewart. Homeostasis in a feed forward loop gene regulatory network motif. *J. Theoretical Biology* **445** (2018) 103–109.

[Andrade et al. (2021)] P.P.A Andrade, J.L.O. Madeira, F. Antoneli. Infinitesimal homeostasis of intracellular copper regulation. In preparation.

[Aoki et al. (2019)] S.K. Aoki, G. Lillacci, A. Gupta, A. Baumschlager, D. Schweingruber, and M. Khammash. A universal biomolecular integral feedback controller for robust perfect adaptation. *Nature* **570** (2019) 533–537.

[Araujo and Liota (2018)] R.P. Araujo and L.A. Liota. The topological requirements for robust perfect adaptation in networks of any size. *Nature Comm.* **9** (2018) 1757.

[Barkai and Leibler (1997)] N. Barkai and S. Leibler. Robustness in simple biochemical networks. *Nature* **387** 913–917 (1997)

[Best et al. (2009)] J. Best, H.F. Nijhout and M. Reed. Homeostatic mechanisms in dopamine synthesis and release: a mathematical model. *Theoretical Biology and Medical Modelling* **6** (21) (2009).

[Cannon (1926)] W.B. Cannon. Physiological regulation of normal states: some tentative postulates concerning biological homeostatic. *Paris: Editions Medicales* p. 91

[Del Vecchio et al. (2018)] D. Del Vecchio, Y. Qian, R.M. Murray, and E.D. Sontag. Future systems and control research in synthetic biology. *Annu. Rev. Control* **45** (2018) 5–17.

[Edgington and Tindall (2018)] M.P Edgington and M.J. Tindall Mathematical analysis of the escherichia coli chemotaxis signaling pathway. *Bull Math Biol* (2018) **80** (4) 758–787

[Ferrell (2016)] J.E. Ferrell. Perfect and near perfect adaptation in cell signaling. *Cell Systems* **2** (2016) 62–67.

[Golubitsky and Stewart (2017)] M. Golubitsky and I. Stewart. Homeostasis, singularities and networks. *J. Math. Biol.* **74** (2017) 387–407.

[Golubitsky and Stewart (2018)] M. Golubitsky and I. Stewart. Homeostasis with multiple inputs. *SIAM J. Appl. Dynam. Sys.* **17** (2) (2018) 1816–1832.

[Golubitsky and Wang (2020)] M. Golubitsky and Y. Wang. Infinitesimal homeostasis in three-node input-output networks. *J. Math. Biol.* pp 1–23 (2020)

[Harary and Palmer (1973)] F. Harary and E.M. Palmer. Graphical enumeration. Academic Press pp.241 (1973)

[Kodama (1993)] H. Kodama. Recent developments in menkes Disease. *J. Inher. Metab.* **16** (1993) pp. 791-799

[Lloyd (2013)] A.C. Lloyd. The regulation of cell size. *Cell* **154** (2013) 1194.

[Lutsenko et al. (2006)] S. Lutsenko, N.L. Barnes, M.Y. Bartee, and O.Y. Dmitriev. Function and regulation of human copper-transporting ATPases. *Physiological Reviews* **87 (3)** (2007) 1011-1046

[Ma et al. (2009)] W. Ma, A. Trusina, H. El-Samad, W.A. Lim, and C. Tang. Defining network topologies that can achieve biochemical adaptation. *Cell* **138** (2009) 760–773.

[Madeira and Antoneli] J. Maderia and F. Antoneli. Homeostasis in networks with multiple input nodes and robustness in bacterial chemotaxis. In preparation.

[Morrison (1946)] P.R. Morrison. Temperature regulation in three Central American mammals. *J Cell Comp Physiol.* **27** (1946) 125–137.

[Mulukutla et al (2014)] Mulukutla BC, Yongky A, Daoutidis P, Hu W-S. Bistability in glycolysis pathway as a physiological switch in energy metabolism. *PLoS ONE* **9** (6) (2014)

[Nijhout et al. (2004)] H.F. Nijhout, M.C. Reed, P. Budu, and C.M. Ulrich. A mathematical model of the folate cycle: new insights into folate homeostasis. *J. Biological Chemistry* **279** (2004) 55008–55016.

[Nijhout and Reed (2014)] H.F. Nijhout and M.C. Reed. Homeostasis and dynamic stability of the phenotype link robustness and plasticity. *Integr Comp Biol.* **54** (2) (2014) 264–75.

[Nijhout et al. (2014)] H.F. Nijhout, J. Best and M. Reed. Escape from homeostasis. *Math. Biosci.* **257** (2014) 104–110.

[Nijhout et al. (2015)] H.F. Nijhout, J.A. Best, and M.C. Reed. Using mathematical models to understand metabolism, genes and disease. *BMC Biology* **13** (2015) 79.

[Nijhout et al. (2018)] H.F. Nijhout, J. Best and M.C. Reed. Systems biology of robustness and homeostatic mechanisms. *WIREs Syst. Biol. Med.* (2018) e1440.

[Qian and Del Vecchio (2018)] Y. Qian and D. Del Vecchio, Realizing 'integral control' in living cells: how to overcome leaky integration due to dilution? *J. R. Soc. Interface* **15** (139) (2018) 20170902.

[Reed et al. (2017)] M. Reed, J. Best, M. Golubitsky, I. Stewart and H.F. Nijhout. Analysis of homeostatic mechanisms in biochemical networks. *Bull. Math. Biol.* **79** (9) (2017) 1–24.

[Reed et al. (2010)] M.C. Reed, A. Lieb and H.F. Nijhout. The biological significance of substrate inhibition: a mechanism with diverse functions. *Bioessays* **32** (5) (2010) 422–429.

[Schneider (1977)] H. Schneider. The concepts of irreducibility and full indecomposability of a matrix in the works of Frobenius, König and Markov. *Linear Algebra Appl.* **18** (1977) 139–162

[Tang and McMillen (2016)] Z.F. Tang and D.R. McMillen. Design principles for the analysis and construction of robustly homeostatic biological networks. *J. Theor. Biol.* **408** (2016) 274–289.

[Wang et al. (2021)] Y. Wang, Z. Huang, F. Antoneli, and M. Golubitsky. The structure of infinitesimal homeostasis in input-output networks. *J. Math. Biol.* To appear.

[Witt et al. (2020)] Witt, Barbara and Schaumlöffel, Dirk and Schwerdtle, Tanja Subcellular localization of copper—cellular bioimaging with focus on neurological disorders. *International Journal of Molecular Sciences.* **21** 7 (2020)

[Wyatt et al. (1999)] J.K. Wyatt, A. Ritz-De Cecco, C.A. Czeisler and D.-J. Dijk, Circadian temperature and melatonin rhythms, sleep, and neurobehavioral function in humans living on a 20-h day. *Amer. J. Physiol.* **277** (1999) 1152–1163.

[Yu et al. (2017)] C.H. Yu, N.V. Dolgova, and O.Y. Dmitriev. Dynamics of the metal binding domains and regulation of the human copper transporters ATP7B and ATP7A. *IUBMB life* **69(4)** (2017) 226-235